BASELINE MODELLING ASSESSMENT REPORT FOR EZAMOKUHLE

Document by:

ARM
AIR RESOURCE MANAGEMENT

Final Report

9 March 2021

Document Title

Client	**Eskom**
Title	**Baseline Modelling Assessment Report for Ezamokuhle**
Our Reference	**ESKPMV-2021-ACTV-01-BMA01**
Issued to Client	**09/03/2021**
Classification	**Company Confidential**

Document Change Record

Revision Number	Date	Description of Revision
00A	1st March 2021	Creation of Document
00B	5th March 2021	Peer Review of Document
01	9th March 2021	Approval of Revised Document

Document Approval

	Name	Designation	Date
Prepared by	Mr A Shamu, Dr G Fourie	Air Quality Specialists	1st March 2021
Reviewed by	Mr F Goede	Executive Head: Air Quality	5th March 2021
Approved by	Mr F Goede	Executive Head: Air Quality	9th March 2021

Contents

LIST OF TABLES

LIST OF FIGURES

EXECUTIVE SUMMARY

Activity 1: Preliminary Air Quality Assessment requires ARM to conduct an initial assessment to ascertain whether the Ezamokuhle airshed is in non-compliance with the National Ambient Air Quality Standards (NAAQS). ARM is utilising a phased three pronged strategy of: firstly a *Status quo air quality trend analysis assessment*; secondly a *Baseline modelling assessment* and finally *Ambient air quality monitoring study* in order to evaluate compliance of the NAAQS at Ezamokuhle. This focus of this report is only on the *Baseline modelling assessment* for Ezamokuhle.

The objective of this study is to firstly assess the baseline modelled ambient concentrations against the NAAQS compliance limits for sulphur dioxide (SO_2), nitrogen dioxide (NO_2) and particulate matter (PM_{10} and $PM_{2.5}$). Secondly the results of this study will be utilised to inform the appropriate & representative placement of the ambient air quality analyzers at Ezamokuhle.

For the study, the US-EPA approved Californian Puff (CALPUFF) modelling suite was utilised. CALPUFF is a non-steady-state, time-and space-dependent Gaussian puff model which is designed to simulate the transport, dispersion, chemical reactions and deposition of gases and particles in the atmosphere. CALPUFF treats emissions as a series of continuous puffs.

An emissions inventory was compiled for the modelling domain which included the following source categories: power generation; residential, vehicle and biomass emissions. The Eskom Majuba Power Station was simulated based on Eskom's reported emissions for the period 2017 to 2019. Vehicular emissions calculated by the DEFF *Integrated Strategy for the Control of Motor Vehicle Emissions* for the Pixley ka Seme Local Municipality were utilised. Residential fuel burning for the modelling domain were estimated based on StatsSA 2011 Census energy use data at the sub-place level for: Ezamokuhle; Daggakraal; Amersfoort and Palmietfontein.The total quantities of fuels being consumed by the households at a sub-place level were estimated based on the typical monthly fuel use figures. The DEFF emission factors for residential fuel burning were then applied to calculate the resultant residential fuel burning emissions for the study. Biomass burning emissions were calculated based on: the total area burned; fuel combustion completeness factors; fuel load and Safari 2000 emission factors.

Based on the emissions inventory above, the CALPUFF modelling suite was utilised to predict the dispersion of the following pollutants: SO_2; SO_4^{2-}; NO_2; NO_3, PM_{10} and $PM_{2.5}$. The total concentrations of particulate matter (PM_{10} or $PM_{2.5}$) were computed as the sum of primary particulate matter concentrations (PM_{10} or $PM_{2.5}$) plus the contribution of concentrations from secondary particulate

matter, including ammonium nitrate and ammonium sulfate. The modelled 99th percentile concentrations for SO_2, NO_2 and PM_{10} were assessed against the NAAQS for sensitive receptors.

The model predicted 99th percentile SO_2, NO_2, PM_{10} and $PM_{2.5}$ concentrations were generally in compliance with the NAAQS in the modelling domain. The trend analysis and polar plots showed that the peak SO_2 concentrations at Ezamokuhle were present at high wind speeds thus indicative of emissions from tall stacks rather than non-buoyant ground-level sources. Conversely at the Eskom Ezamokuhle station, high NO_2 concentrations occur under stable atmospheric conditions when non-buoyant ground-level sources are important. The time variation plot at Ezamokuhle explicitly reveals that the variability of NO_2 concentrations are conditioned by vehicle emissions. Whilst the particulate matter morning and afternoon peaks are a typical profile for residential fuel burning.

The prioritisation of air quality hotspots for Ezamokuhe was ranked on the basis of modelled air quality impacts. This ensured that the areas that potentially pose the greatest risk to human health and the environment were identified for placement of the E-BAM particulate analysers. The highest predicted modelled concentrations for Ezamokuhle occur in China 2 and Roestein. Subsequently a total of eight air quality hotspots located in China 2 & Roestein have been identified for optimum placement of the E-BAM analysers.

Although atmospheric dispersion models are indispensable in air quality assessment studies, their limitations should always be taken into account. The model validation exercise demonstrated that the model performance for SO_2 at the Eskom Ezamokuhle station is satisfactory whilst the model under-predicted NO_2 and PM_{10}. However it must be noted that the analysis of the ambient air quality monitoring data has indicated that both NO_2 and $PM_{2.5}$ are dominated by non-buoyant localised ground-level sources. NO_2 is conditioned by localised vehicle emissions whilst $PM_{2.5}$ is attributable to localised residential burning. For this study, the major roads were modelled and the local roads were excluded due to the lack of localised emissions data and similarly Stats SA data was utilised at a sub-place level to model $PM_{2.5}$ residential burning emissions. However the granularity of this emissions data was not sufficient to cover these localised emission source catergories. Although the model under-predicted at the Eskom Ezamokuhle station, the modelled performed within the acceptable range at the Eskom Majuba ambient station. Nonetheless, it must be noted that *for Activity 12: Atmospheric Dispersion Modelling* a comprehensive emissions inventory will be developed to account for these localised sources (vehicles, local roads and residential fuel use).

In summary, the results of this baseline modelling study has identified air quality hotspots in China 2 and Roestein for the optimum placement of the E-BAM analysers. Additionally the study has

highlighted the role of non-buoyant localised ground-level sources in the Ezamokuhle airshed & the need to develop a bottom-up emissions inventory to account for these localised sources.

INTRODUCTION

1.1 PROJECT BACKGROUND

Air Resource Management (Pty) Ltd (*herein referred to as* ARM) is supporting Eskom's Planning, Monitoring and Verification (PMV) Project at Ezamokuhle (Figure 1). In accordance with the scope of work, *Activity 1: Preliminary Air Quality Assessment* requires ARM to conduct an initial assessment to ascertain whether the Ezamokuhle airshed is in non-compliance with the National Ambient Air Quality Standards (NAAQS). ARM is utilising a phased three pronged strategy (Figure 2) of: firstly a *Status quo air quality trend analysis assessment*; secondly a *Baseline modelling assessment* and finally *Ambient air quality monitoring study* in order to evaluate compliance of the NAAQS at Ezamokuhle. This focus of this report is only on the *Baseline modelling assessment* for Ezamokuhle.

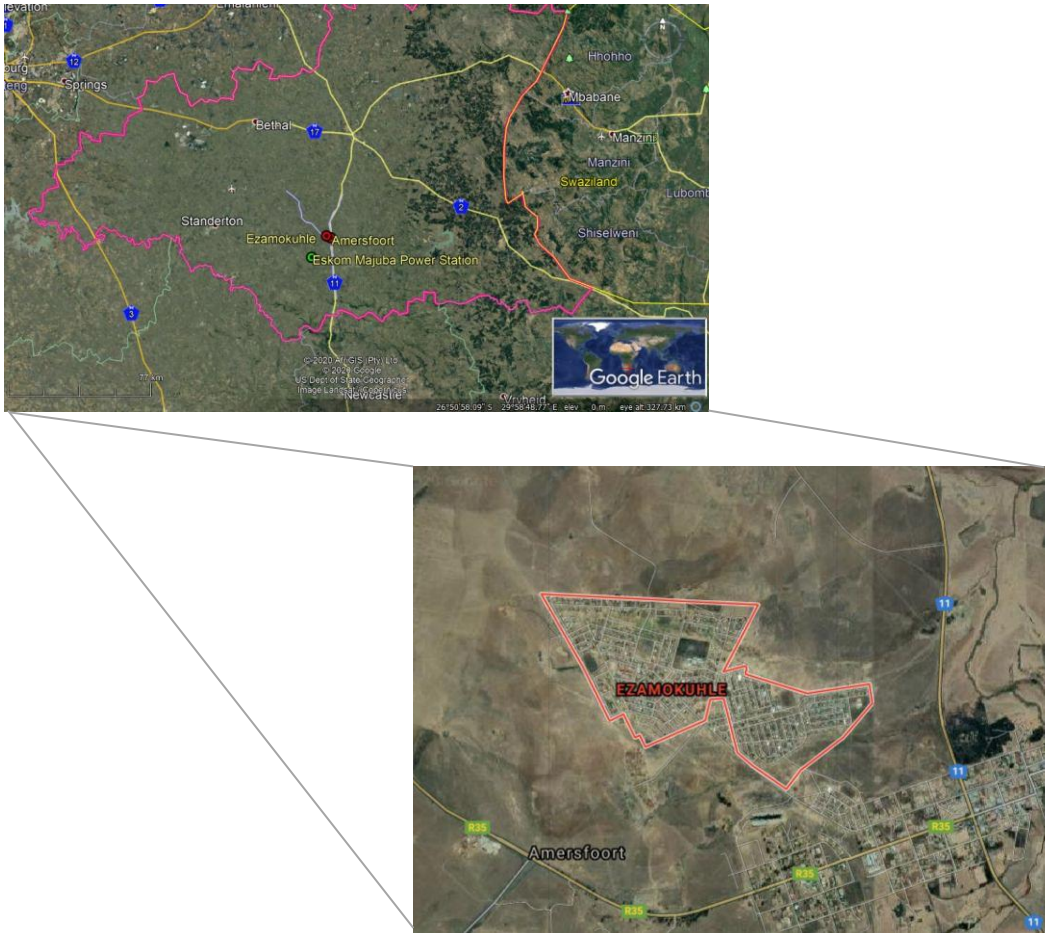

Figure 1: Locality Map for Ezamokuhle

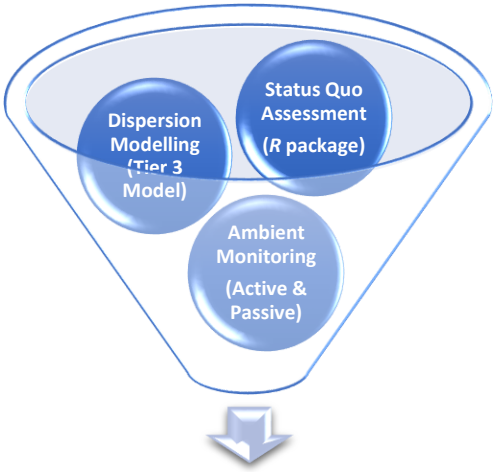

Figure 2: Strategy to evaluate NAAQS non-compliance for Ezamokuhle

1.2 Study Objective

The purpose of this study is to firstly assess the modelled ambient concentrations against the NAAQS compliance limits (Table 1) for sulphur dioxide (SO_2), nitrogen dioxide (NO_2) and particulate matter (PM_{10} and $PM_{2.5}$). Secondly the results of this study will be utilised to inform the appropriate & representative placement of the ambient air quality analysers at Ezamokuhle.

Table 1: NAAQS (DEFF, 2009)

Pollutant	Average Period	Concentration	Frequency of Exceedance	Compliance Date
Nitrogen Dioxide (NO_2)	1 hour	106 ppb	88	Immediate
	1 year	21 ppb	0	Immediate
Ozone (O_3)	8 hour	61 ppb	11	Immediate
Inhalable particulate matter less than 2.5 µm in diameter ($PM_{2.5}$)	24 hour	40 µg/m^3	4	Immediate until 31 December 2029
	24 hour	25 µg/m^3	4	1 January 2030
	1 year	20 µg/m^3	0	Immediate until 31 December 2029
	1 year	15 µg/m^3	0	1 January 2030
Inhalable particulate matter less than 10 µm in diameter (PM_{10})	24 hour	75 µg/m^3	4	Immediate
	1 year	40 µg/m^3	0	Immediate
Sulphur Dioxide (SO_2)	10 minutes	190 ppb	526	Immediate
	1 hour	134 ppb	88	Immediate
	24 hour	48 ppb	4	Immediate
	1 year	19 ppb	0	Immediate

1.3 Report Structure

A general description of Ezamokuhle is presented in Section 2 which describes the: topography and land use; climatology and meteorology & historical ambient air quality information. The modelling methodology and emissions inventory is outlined in Section 3. The results and discussion contained in Sections 4 provides an analysis of the model predicted concentrations. Section 5 evaluates the performance of the modelled values. Conclusions for the baseline assessment are presented in Section 6.

GENERAL DESCRIPTION OF AREA

2.1 LOCATION

The township of Ezamokuhle lies adjacent to the town of Amersfoort in Mpumalanga Province, South Africa (Figure 1). According to the Census 2011 data, Ezamokuhle has an area of 6.21 km^2 with a population of 10,293 (1,657.64 per km^2) and has 2,956 (476.05 per km^2) households (StatsSA, 2012).

2.2 TOPOGRAPHY & LAND USE

2.2.1 TOPOGRAPHY

The Australian CSIRO Atmospheric Research Division, TAPM model was utilised to determine the topographical terrain map for the study area (Figure 3). The global terrain height and land use datasets are sourced from the US Geological Survey (USGS), Earth Resources Observation Systems (EROS) Data Center Distributed Active Archive Center (EDC DAAC). The topography of the area is relatively flat with generally uniform terrain.

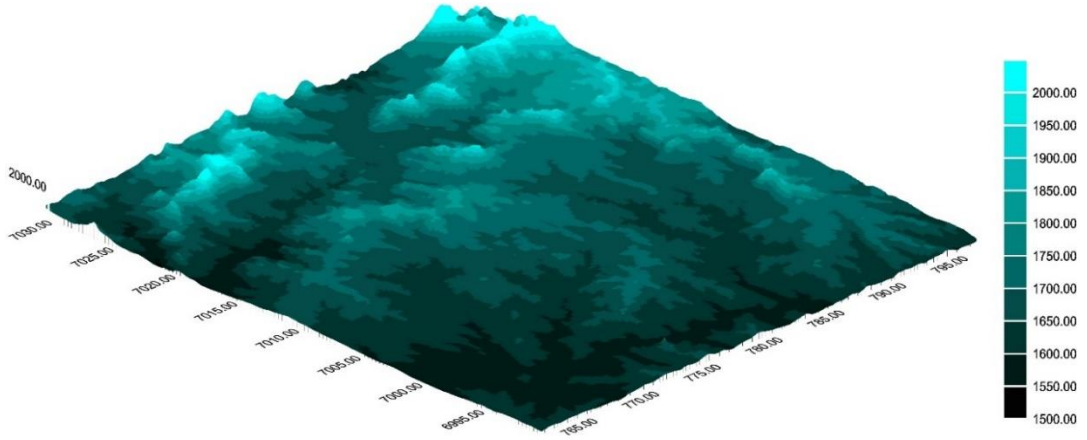

Figure 3: Topography of the Study Area

2.2.2 LAND USE

For atmospheric dispersion modelling an understanding of the land use information is critical. Based on this information, appropriate chemical transformation mechanisms; dispersion coefficients; albedo; surface moisture and surface roughness are selected for the modelling assessment. The classification

of a site as urban or rural is based on the Auer method specified in the US EPA guideline on air dispersion models (US EPA, 2005). The classification scheme is based on the activities within a 3 km radius of the emitting source.

From the Auer's method, areas typically defined as rural include residences with grass lawns and trees; large estates; metropolitan parks and golf courses; agricultural areas; undeveloped land and water surfaces. An area is defined as urban if it has less than 35% vegetation coverage or the area falls into one of the use types in Table 1. A land cover map of the study area is presented in Figure 4. Based on the Auers assessment method detailed above, the study area is classified as rural.

Table 2: Land types, use and structures and vegetation cover

Urban Land Use		
Type	**Use and Structures**	**Vegetation**
I1	Heavy industrial	Less than 5 %
I2	Light/moderate industrial	Less than 5 %
C1	Commercial	Less than 15 %
R2	Dense single / multi-family	Less than 30 %
R3	Multi-family, two-story	Less than 35 %

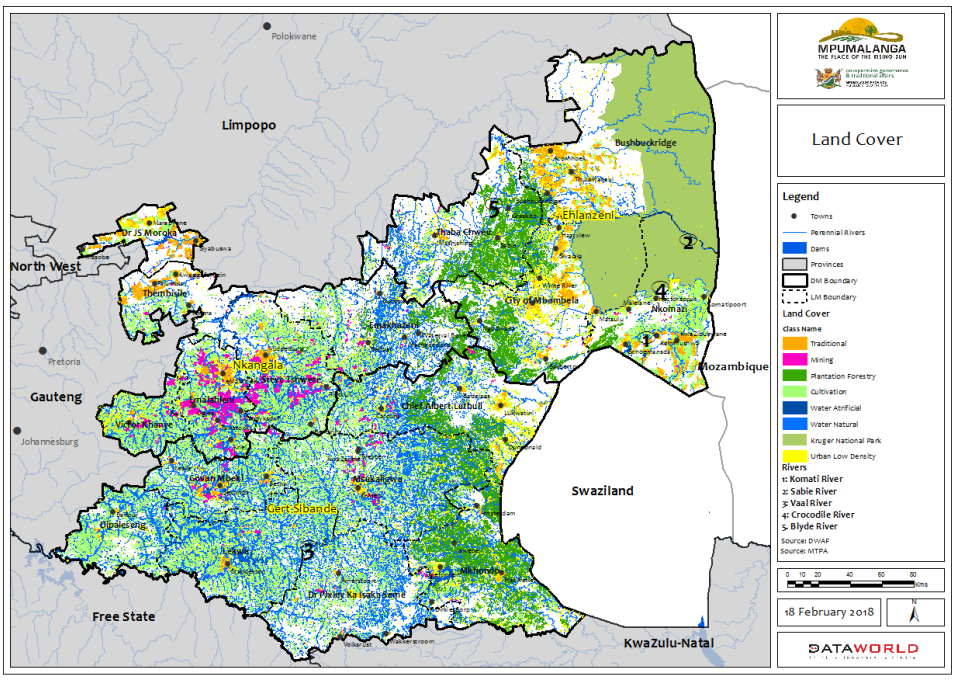

Figure 4: Land cover for Mpumalanga (Source: Mpumalanga Spatial Development Framework, 2019)

2.3 Climate & Meteorology

The Highveld experiences a temperate climate with dry winters according to the Köppen Climate Classification system. The winters are mild and dry, but cold at night. Rainfall occurs in summer. The rain is largely due the development of low-pressure troughs over the central plateau in summer whilst the dry winters are due to the dominant subtropical high pressure. The temperate temperatures are attributed to the relatively high altitude (DEFF, 2010).

2.3.1 Rainfall & Temperature

The region received a mean annual rainfall of ~1.7 mm for the period 2018 to 2020. Rainfall occurs predominantly from October to April, with the maximum in summer (December). The mean monthly rainfall totals recorded at Ezamokuhle are illustrated in Figure 6.

Average temperatures for the area are mild throughout the year with slightly cooler temperatures in winter. The long term average (2018-2020) maximum temperature is 27°C in summer and 20.2°C in winter, with extreme maxima of 34.8°C in summer and 29.8°C in winter. The long term minimum, maximum and mean temperatures observed at the Eskom Ezamokuhe station is illustrated below by Figure 6.

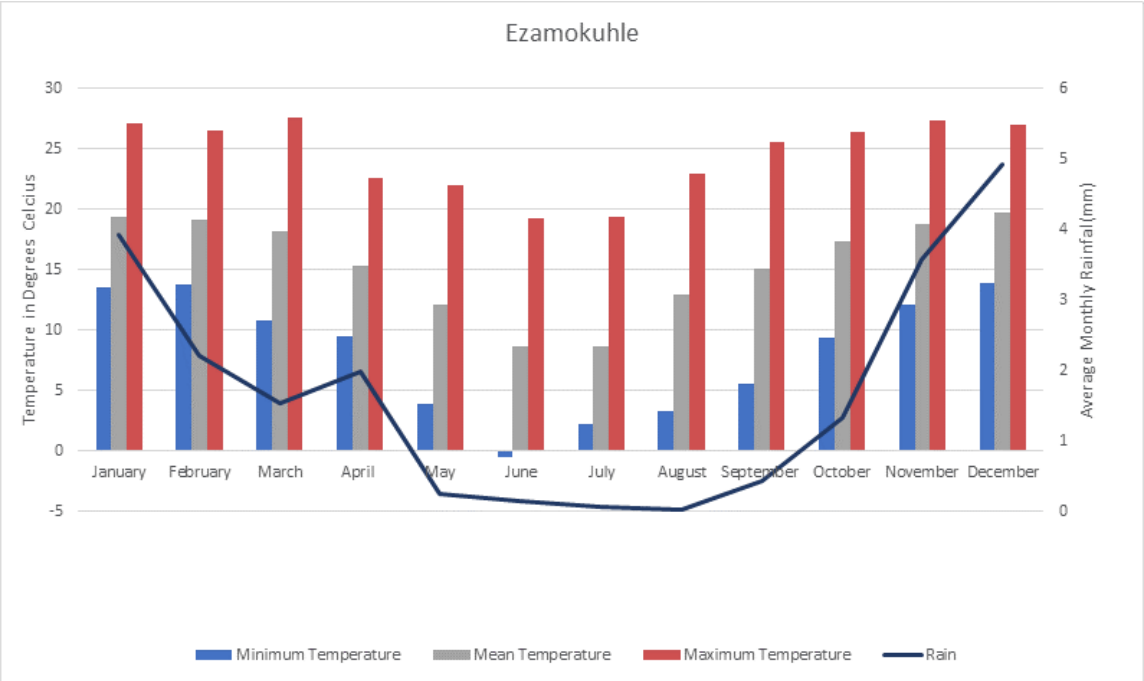

Figure 5: Average maximum and minimum temperatures and average monthly rainfall

2.3.2 Surface & Near-Surface Winds

Air quality is strongly influenced by meteorology. Meteorological mechanisms govern the dispersion, transformation, and eventual removal of pollutants from the atmosphere (Seaman, 2000). The analysis of hourly average meteorological data is necessary to facilitate a comprehensive understanding of the dispersion potential of the site. The horizontal dispersion of pollution is largely a function of the wind field. The wind speed determines both the distance of downward transport and the rate of dilution of pollutants. The wind rose is a very useful way for showing how wind speed and wind direction conditions vary by year.

Wind Direction

At the Eskom Ezamokuhle air quality station the average wind speed for the period 2018 to 2019 (Figure 6) was recorded at 2.93 meters/second with calm condition 0.1%. Calm condition means that wind speed is recorded at zero meter/second (Carlaw, 2015). The predominant wind directions were both easterly (~ 15% frequency of occurrence) followed by westerly (~ 14% frequency of occurrence) with maximum wind speed of 6 – 13.7 meters/second.

The wind speed and direction data also demonstrate a seasonal signal Eskom Ezamokuhle air quality station (Figure 7). For the spring and summer months, the average wind speed for was recorded between ~ 3.1 to 3.4 meters/second with the predominant wind direction been an easterly wind (~ 15% to 20% frequency of occurrence for the period) followed by both a westerly wind and a north-westerly wind (~ 10% frequency of occurrence). Whilst for the autumn and winter winds, the average wind speed for was recorded between ~ 2.4 to 2.7 meters/second with the predominant wind direction been a westerly wind (~ 14% to 25% frequency of occurrence for the period) followed by a north-westerly wind (~ 10% to 15% frequency of occurrence for the period).

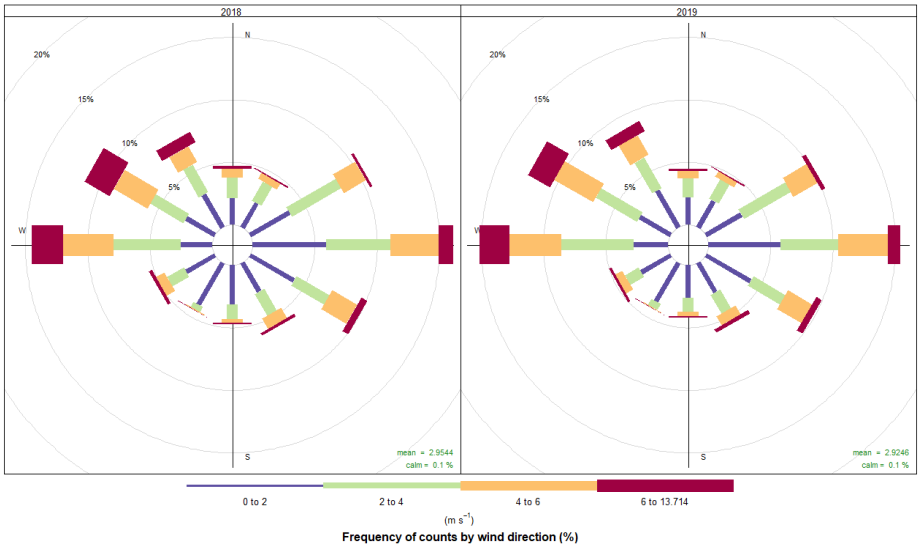

Figure 6: Annual wind rose for the Eskom Ezamokuhle station for the period 2018 to 2019

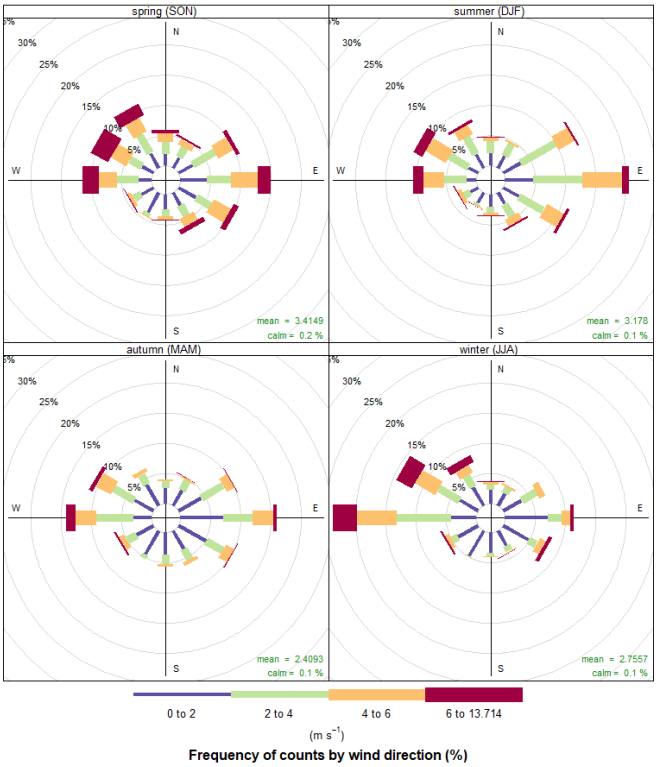

Figure 7: Seasonal wind rose for the Eskom Ezamokuhle station for the period 2018 to 2019

WIND SPEED

Wind drives the atmospheric transport and strongly affects vertical air mixing and thus the ventilation of the urban air (Grundstrom et al., 2015). Stagnant atmospheric conditions with calm, clear weather often lead to stable atmospheric stratification which consequently leads to poor air quality (Delaney and Dowding, 1998; Janhall et al., 2006; Olofson et al., 2009). Low wind speeds deteriorate air quality with respect to pollutants emitted near the ground due to restricted air ventilation (Jones et al., 2010). In contrast higher wind speeds are associated with increased dispersion and mixing of atmospheric pollutants which may result in low ambient pollution concentrations.

Figures 8 illustrates the monthly wind speed average for the Eskom Ezamokuhle station. At the Eskom Ezamokuhle stations the period January until May the wind speed pattern shows a decrease from with low averages recorded until July. This is associated with less mixing and dispersion of pollutants thus resulting in elevated ambient concentrations in winter (Liebenberg, 1999).Conversely, there is an increase in wind speeds recorded from August until December. This is associated with increased dispersion and mixing of atmospheric pollutants which may result in lower ambient pollution concentrations.

Figure 9 illustrate the diurnal wind speed average for the Eskom Ezamokuhle station. For all stations, lower wind speeds are logged from 19h00 until 08h00. This is associated with elevated atmospheric pollution concentrations due to less mixing and dispersion. The wind speeds then increase from 09h00 until 17h00. This is associated with less pollution concentrations influenced by an increase in the mixing and dispersion of atmospheric pollutants (Liebenberg, 1999).

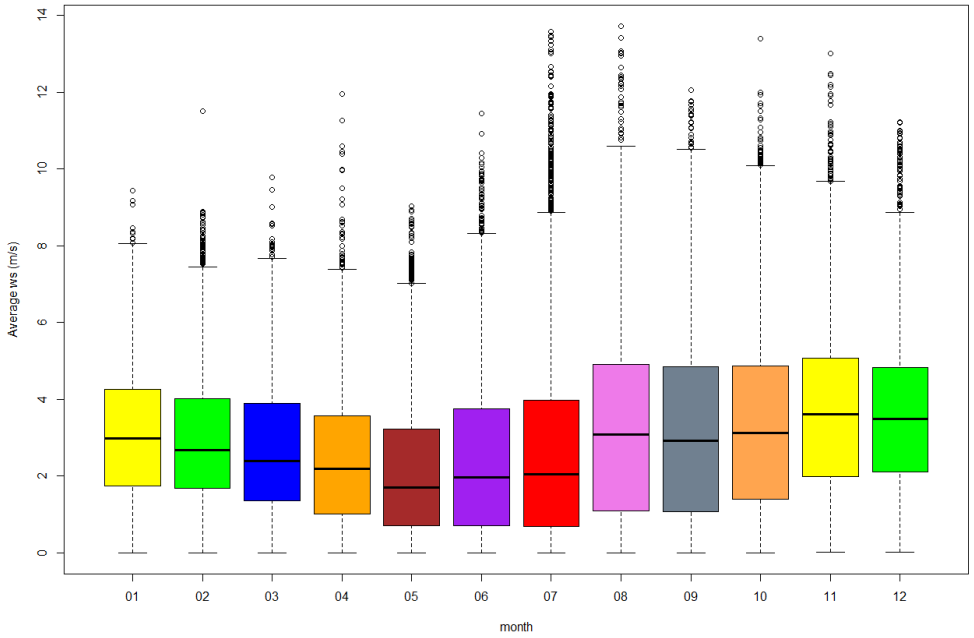

Figure 8: Monthly wind speed averages for the Eskom Ezamokuhle Station (whisker & box indicates interquartile range, diamond indicate outliers and the bars indicate the min and max value)

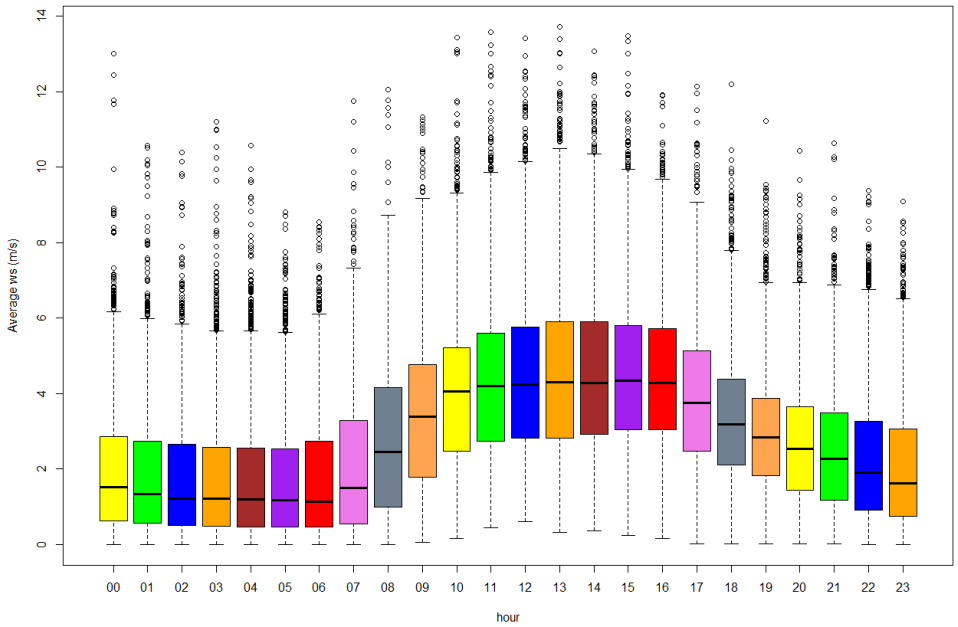

Figure 9: Diurnal wind speed averages for the Eskom Ezamokuhle Station (whisker & box indicates interquartile range, diamond indicate outliers and the bars indicate the min and max value)

2.3.3 Dispersion Potential

The extent to which synoptic systems and weather disturbances impact on the dispersion potential of the atmosphere depends on the height and persistence of elevated inversions. Elevated inversions reduce the height at which pollutants are able to mix, and consequently results in the concentration of pollutants below their bases. These inversions therefore play a key role in the recirculation of pollutants as well as controlling the long-range transport.

The southern African subcontinent is under the influence of a semi-permanent sub-tropical anticyclone. They are dominant in mid-winter with a frequency of 80% as opposed to 20% in summer (Garstang et al., 1996). These high pressure systems are associated with large-scale subsidence inversions which has a considerable influence on the accumulation of trace gases and aerosols in the troposphere (Garstang et al., 1996; Swap and Tyson, 1999). The presence of subsidence induced semi-permanent absolutely-stable layers at altitudes of approximately 700 hPa (~3 km), 500 hPa (~5 km) and 300 hPa (~7 km) (Figure 10), were identified over southern Africa by Cosijn and Tyson (1996) and Freiman and Tyson (2000). The horizontal and vertical transport of aerosols between the surface and the tropopause is controlled by these stable layers (Garstang et al, 1996). The lower level elevated subsidence inversion is significant in that it represents a persistent cap impeding the upward mixing of air pollutants (DEFF, 2007).

Convective activity hinders the formation of inversions. Whilst cyclonic disturbances are usually associated with the dissipation of inversions, pre-frontal conditions tend to lower the base of the elevated inversion, thus reducing the mixing depth. After the passage of cold front, there is a gradual increase in the mixing depth (Scott and Diab, 2000).

For Ezamokuhle, the dispersion potential is anticipated to be better during the day due to higher daytime temperatures and a higher frequency of moderate wind speeds. Additionally due to: a higher frequency of stronger winds; higher rainfall; stronger thermal mixing; weaker & less persistent night-time temperature inversions the summer months will have a better dispersion potential than the winter months.

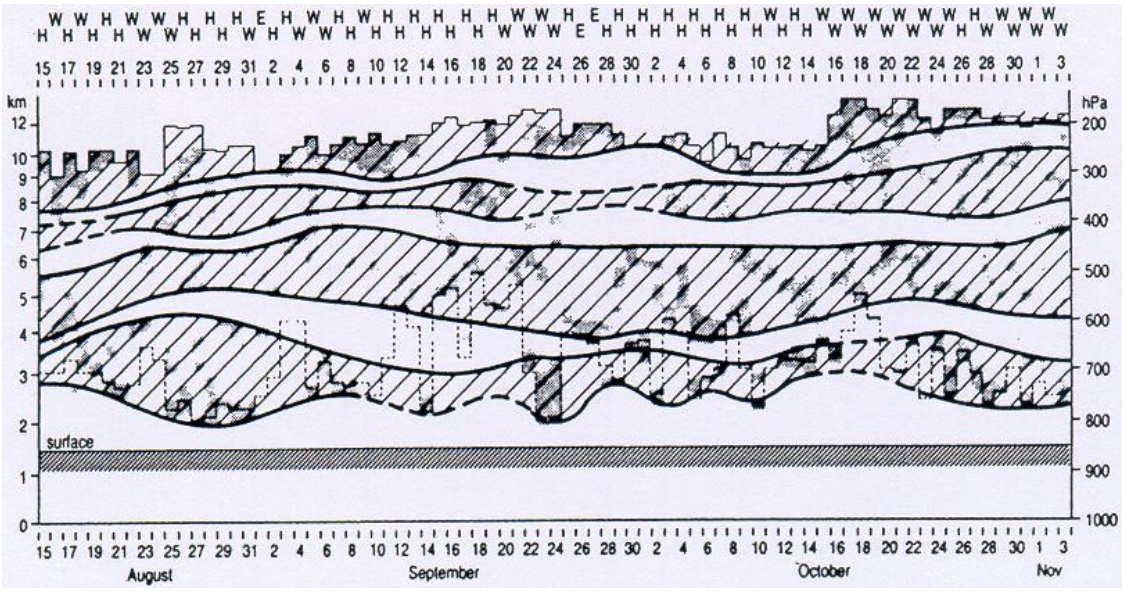

Figure 10: Daily variation of absolutely stable layers over Pretoria (southern Africa) during SAFARI-92. Stippled boxes indicate the height and depth of stable layers. Envelopes of continuous and discontinuous stable layers are indicated by cross-hatched regions enclosed by solid and dashed lines respectively. Light dashed lines depict the height of the 1200UT mixing depth. Circulation class for each day is shown by H (continental high), W (westerly disturbance) and E (easterly disturbance) (Source: Garstang et al., 1996: p 23724)

2.4 AMBIENT AIR QUALITY MONITORING ANALYSIS

The Openair air quality model was utilised to statistically analyse the semi-empirical mathematical relationships between air pollutant concentration and meteorological factors for the Eskom Ezamokuhle station for the period 1 January 2018 to 31 December 2019.

2.4.1 TREND ANALYSIS PLOT

The trend analysis (mean with 95% confidence interval) of ambient pollutant concentrations measured at the Eskom Ezamokuhle station show the variation of these pollutants over daily, weekly and annual cycles for the period 2017 to 2018.

SO_2 (Figure 11) show a typically industrial signature with increased SO_2 concentrations at just around midday due to the break-up of an elevated inversion layer, in addition to the development of daytime convective conditions causing the plume to be brought down to ground level relatively close to the point of release from tall stacks. The winter (June, July and August) elevation of SO_2 shows the contribution of residential fuel burning to the ambient SO_2 concentrations at the Eskom Ezamokuhle station. It's evident there is a second less pronounced peak compared to midday that occurs at 18:00

in winter (peaking in the months of June and July) thus indicating the impact of residential fuel burning emissions.

The Ezamokuhle NO_2 results (Figure 11) explicitly reveal that the variability of this pollutant concentration is conditioned by vehicle emissions. Daily and weekly variation corresponds to the cyclical nature of traffic volume with marked peaks in concentration on weekdays around the early-morning and late-afternoon rush-hours. Figure 11 shows NO_2 concentrations plotted by time-of-day for Ezamokuhle. It shows a clear rise in concentrations with the peak of the morning rush-hour at around 06:00 and a second less marked rise with the evening rush-hour peaking at around 18:00. The winter elevation of NO_2 shows the contribution of residential fuel burning to the ambient NO_2 concentrations at the Eskom Ezamokuhle and Majuba stations.

O_3 in the lower troposphere forms through the reaction between oxides of nitrogen and volatile organic compounds in the presence of the ultraviolet portion of sunlight (<420nm) (Tienhoven et al., 2005). O_3 (Figure 11) show a strong diurnal & seasonal variation. The surface ozone concentrations increase from a minimum near sunrise to a maximum in the afternoon (around 15:00), then decrease again to the early morning minimum throughout the entire week (Figure 11). The highest concentrations occur around September which coincides with the biomass burning season in Southern Africa. Biomass burning is seasonal and occurs almost exclusively during the winter and into spring, from July to September (Silva et al., 2002).

The particulate matter morning peak occurs at 07:00 whilst the evening peak occurs at 18:00. This is a typical profile for residential fuel burning. The morning peaks reduces towards midday as the inversion layer rises & improves the mixing height of the planetary boundary layer. It's evident there is a third less pronounced peak that occurs at midday due to the break-up of an elevated inversion layer, in addition to the development of daytime convective conditions causing the plume from tall stack emissions to be brought down to ground level. Monthly variation of particulate matter shows elevated concentrations during early winter months to early spring (May to September) due to the greater contribution from domestic fuel burning, dust from uncovered soil and the lack of the settling influence of rainfall.

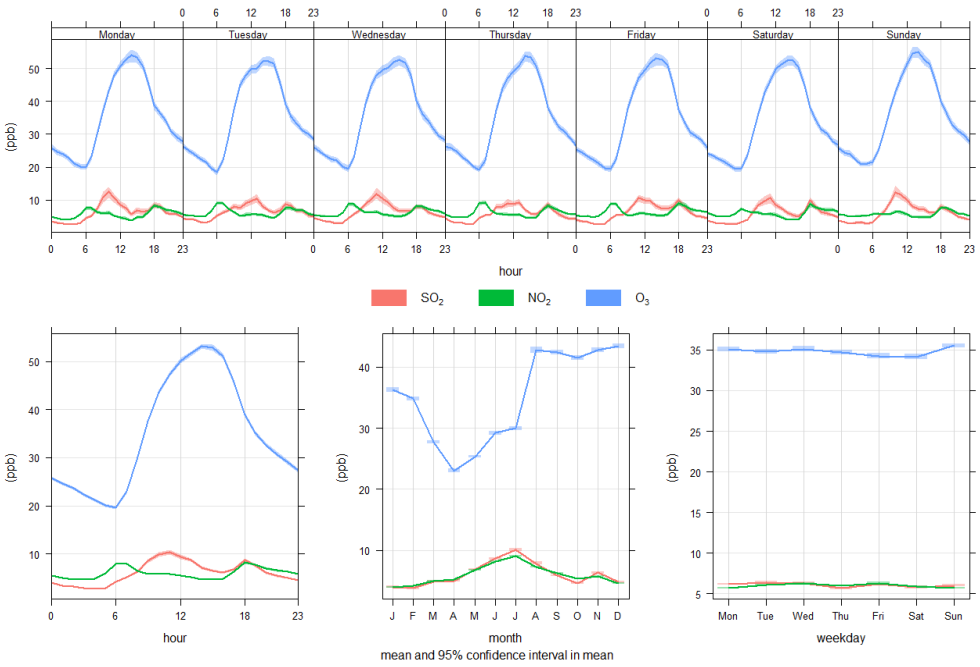

Figure 11: Mean pollutant concentrations in ppb for the Eskom Ezamokuhle air quality station calculated for hourly mean during weekdays and a single day, monthly, and daily mean (2018–2019).

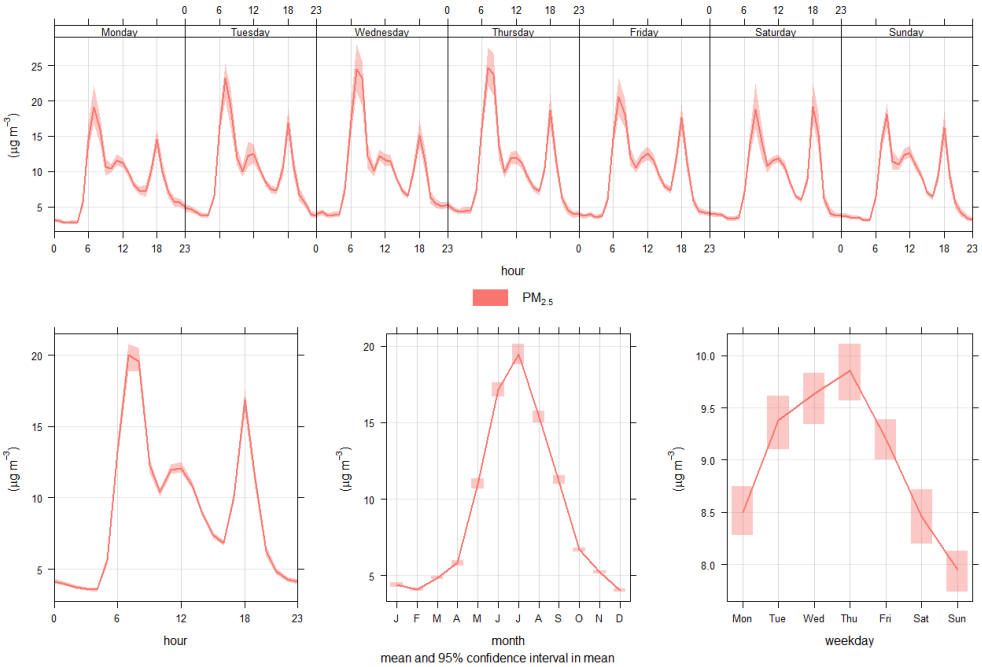

Figure 12: Mean pollutant concentrations in ug/m3 for the Eskom Ezamokuhle air quality station calculated for hourly mean during weekdays and a single day, monthly, and daily mean (2018–2019).

2.4.2 TIME SERIES ANALYSIS

A summary of the ambient data measured at the Eskom Ezamokuhle station for the period 2018 – 2019 is provided in Table 3.

Table 3: Summary of ambient air quality measurements for the Eskom Ezamokuhle station

Station	Year	Maximum Measured Pollutant Measurement			
		SO_2 (ppb)		NO_2 (ppb)	$PM_{2.5}$ (ug/m^3)
		Hourly	Daily	Hourly	Daily
Ezamokhule	**2018**	224	29	53	61
	2019	81	27	54	51

*Exceedances of the NAAQS is shown in red text

The time-series graphs (Figure 13 to 16) summarise the observed concentrations of SO_2, NO_2, and $PM_{2.5}$ at the Eskom Ezamokuhle monitoring station for the years 2018 to 2019. The hourly 99th percentiles for SO_2 were only above the limit value of 134 ppb for 3 occasions in 2018 (Figure 13). These exceedance occur in the months of January, April and August just around midday. Additionally the polar plot for the station (Figure 17) further show a typically industrial signature with increased SO_2 concentrations as just before midday due to the break-up of an elevated inversion layer, in addition to the development of daytime convective conditions causing the plume to be brought down to ground level relatively close to the point of release from tall stacks. Thus these exceedances are likely due to the impact of an elevated emission source. It's evident from Figure 14 that the daily SO_2 concentrations were well below the NAAQS limit value of 48 ppb for the entire period. Similarly Figure 15 clearly shows that there were no recorded exceedances of the hourly NO_2 NAAQS standard of 106 ppb.

The NAAQS for the daily $PM_{2.5}$ limit (40 ug/m3) was exceeded for 1 occasion in 2018 (Figure 16) which occurs at 7pm thus indicating the impact of a residential fuel burning source. The 2019 NAAQS for $PM_{2.5}$ was exceeded in the winter months, with the peak concentrations occurring at 08:00 whilst the evening peak occurs at 18:00, a typical profile for residential fuel burning.

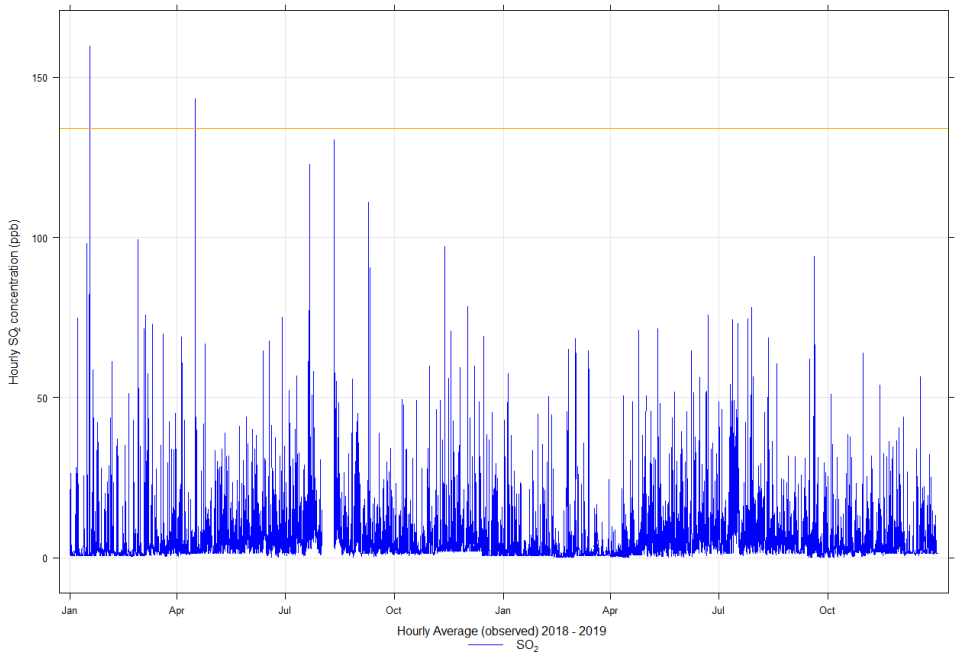

Figure 13: Time series for the hourly SO_2 ground level concentrations measured at the Eskom Ezamokuhle ambient air quality monitoring station (2018-2019)

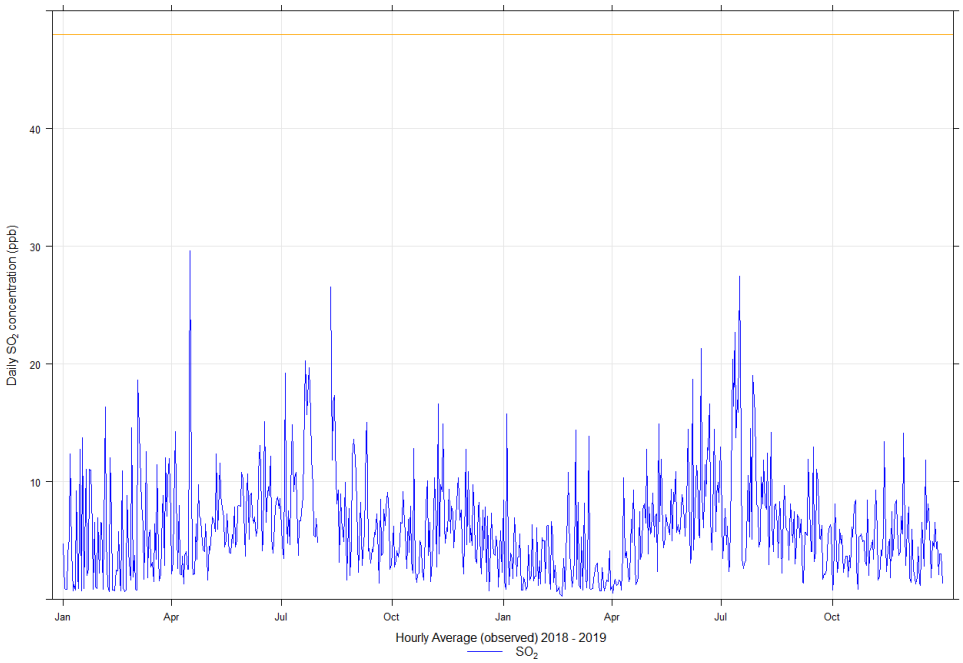

Figure 14: Time series for the daily SO_2 ground level concentrations measured at the Eskom Ezamokuhle ambient air quality monitoring station (2018-2019)

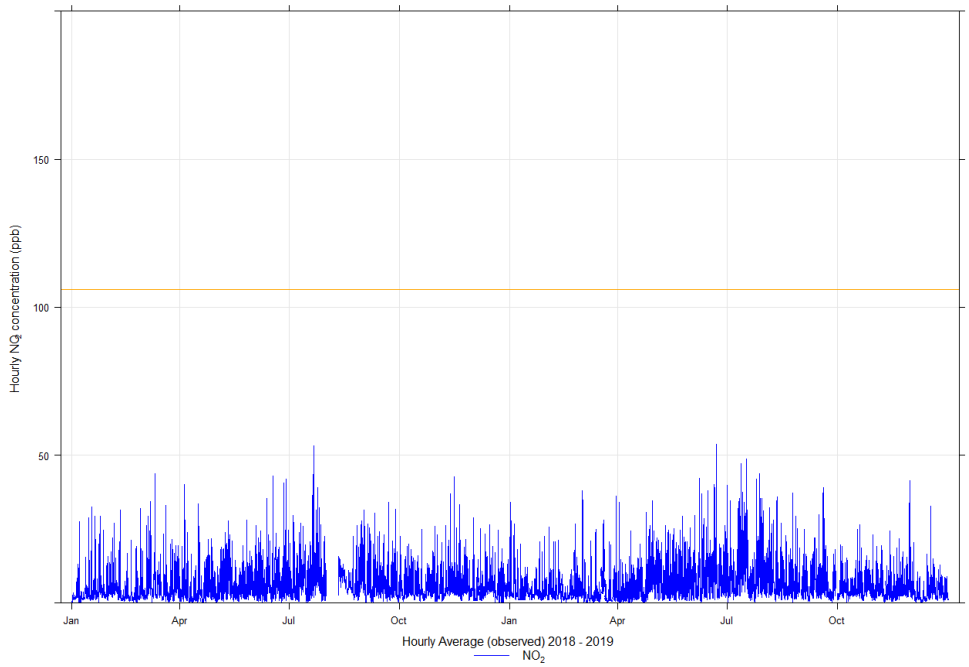

Figure 15: Time series for the hourly NO_2 ground level concentrations measured at the Eskom Ezamokuhle ambient air quality monitoring station (2018-2019)

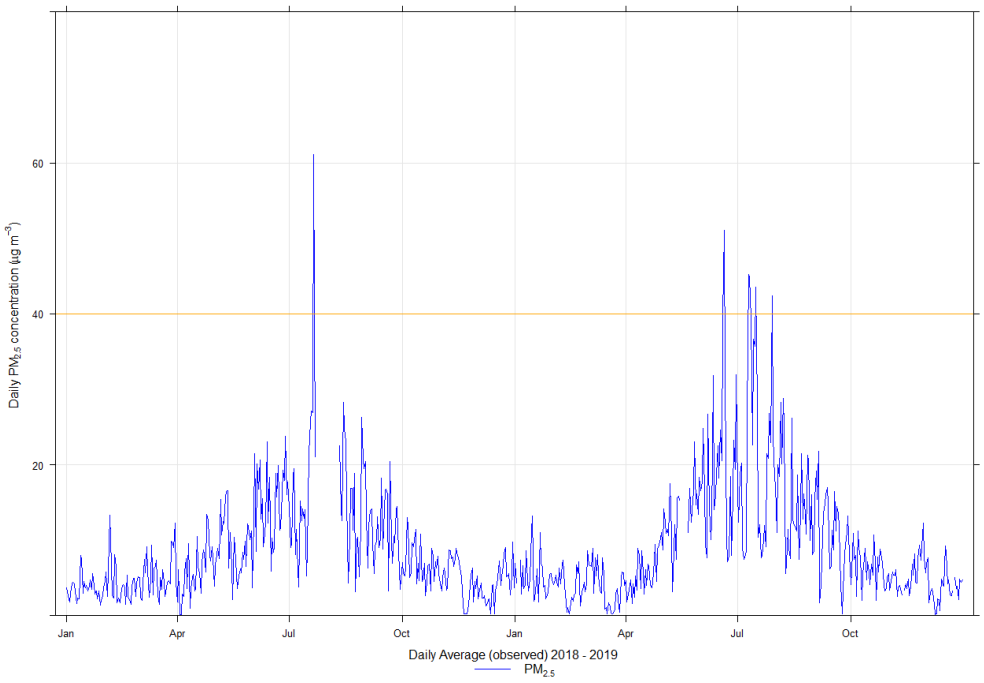

Figure 16: Time series for the daily $PM_{2.5}$ ground level concentrations measured at the Eskom Ezamokuhle ambient air quality monitoring station (2018-2019)

2.4.3 EMISSION SOURCE CONTRIBUTION

Source-specific information can be extracted if analyses are performed using a subset of the data that has been 'conditionally-selected' to exclude superimposed impacts from non-relevant sources (Malby et al., 2013). A common method for source characterisation is the use of bivariate polar plots (Carslaw et al., 2006; Westmoreland et al., 2007; Carslaw and Beevers, 2013; Uria Tellaetxe and Carslaw, 2014).

Figures 17 to 19 shows the bivariate plots for the Eskom Ezamokuhle station conditioned for the mean pollutant concentration. The SO_2 concentrations observed at the station (Figure 17) show two distinct wind directions, namely from the south-west and the north-west. High concentrations present at high wind speeds are indicative of emissions from stacks rather than non-buoyant ground-level sources. Hence the higher SO_2 concentrations associated with the south-westerly winds are most likely due to emissions from the Eskom Majuba station. Similarly the SO_2 concentrations from the north-west indicates a distinct tall stack emission source located in Secunda.

Figure 18 shows the bivariate NO_2 polar plot for the Eskom Ezamokuhle station. The highest concentrations occur under very low wind speed conditions from the south-west. These high concentrations occur under stable atmospheric conditions when non-buoyant ground-level sources are important such as road transport emissions. Figure 11 confirms that these NO_2 concentrations are the likely impact of vehicle emissions. The bivariate polar plot also shows are area of high concentration to the north-west that occur at high wind speeds, possibly corresponding to the activities of a tall stack emission source located in Secunda.

Elevated particulate concentrations at Ezamokuhle show contributions from the north-west and the south-east at higher (between 8 and 14 m/s) wind speeds (Figure 49). At low wind speeds the symmetrical plot shows a localised contribution, most likely the result of residential fuel burning (Figure 12).

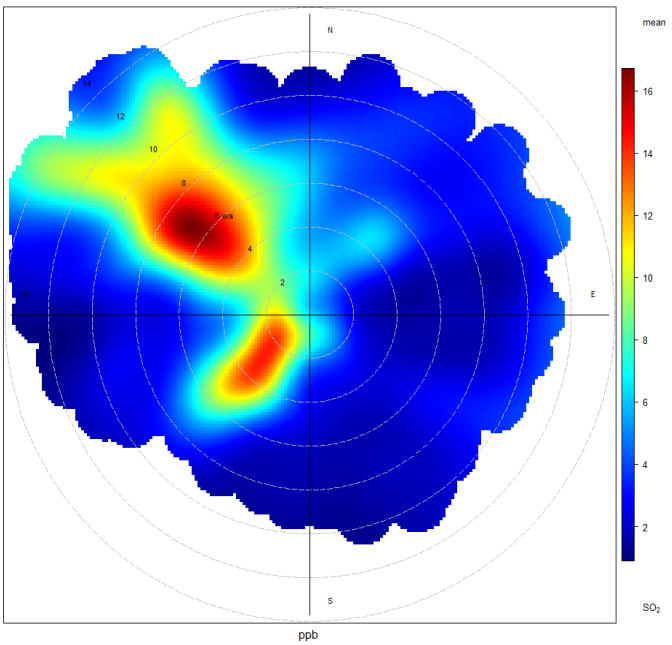

Figure 17: Polar plot of hourly mean SO_2 concentration at the Eskom Ezamokuhle Station for 2018 to 2019

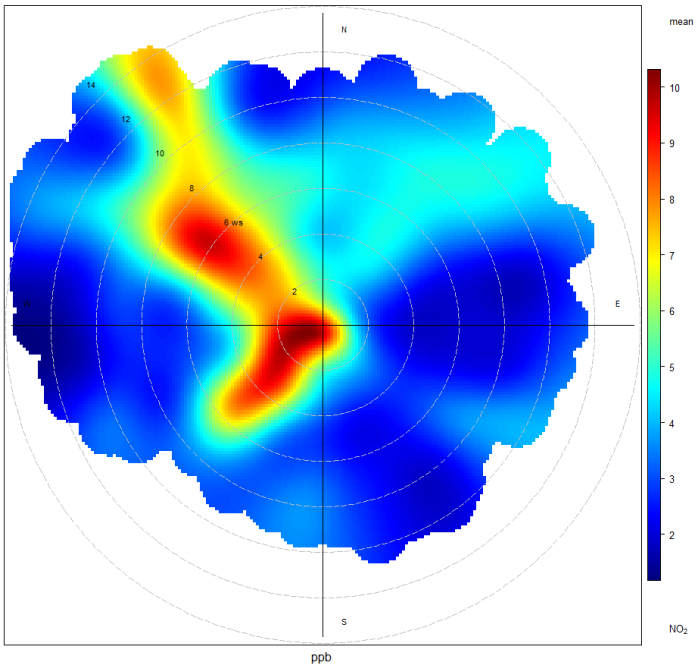

Figure 18: Polar plot of hourly mean NO_2 concentration at the Eskom Ezamokuhle Station for 2018 to 2019

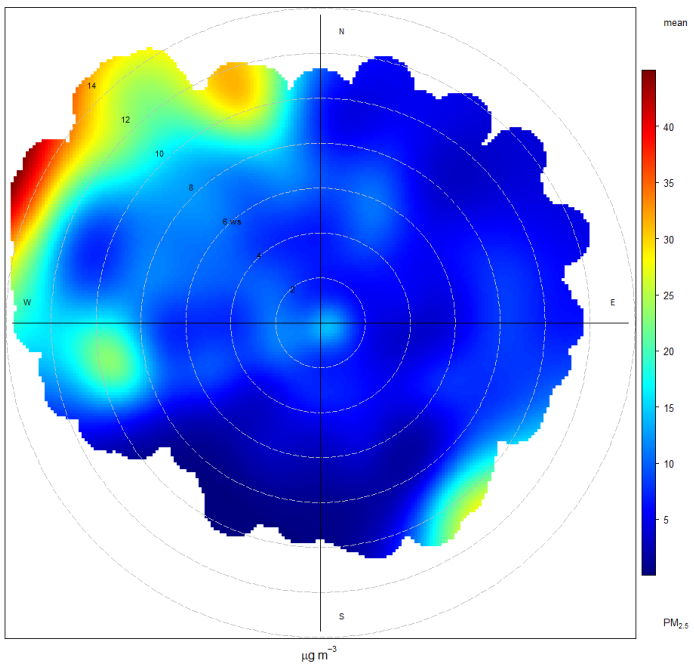

Figure 19: Polar plot of hourly mean $PM_{2.5}$ concentration at the Eskom Ezamokuhle Station for 2018 to 2019

MODELLING PROCEDURE

3.1 BACKGROUND

Models have been used for decades to approximate physical systems and make estimates about the nature of the system under study (US EPA, 2004). Graedel and Crutzen (1997) have shown that it has become common practice in the environmental science field to describe complex systems of interacting physical, chemical, and biological processes through the design of numerical models. For example, mathematical models are often utilised for assessing air pollution impacts in order to gain a better insight into this multidimensional (Denzer, 2004) and multidisciplinary (Wang, 2005) challenge.

Atmospheric dispersion models utilise mathematical equations that simulate the physics (Briggs, 1975; Gifford, 1960; Pasquill, 1983; Turner, 1970) and chemistry (Seinfeld and Pandis, 1998) that control the transport and transformation of pollutants in the atmosphere. They provide a means of estimating air pollutant concentrations and particle deposition in the ambient environment based on information on emissions and the prevailing meteorology (Chen et al., 2001; NSW, 2004).

3.2 ASSESSMENT LEVEL PROPOSED AND JUSTIFICATION

A number of dispersion models to be used in regulatory applications in South Africa. The suitability for a particular model for an air quality assessment will vary depending on the: scope of the study; the objectives of the modelling effort; technical factors and the level of risk associated with the project. According to the Regulations Regarding Air Dispersion Modelling (Gazette No 37804, 2014), tiered approach in the selection of an air dispersion model is recommended. It's recommended that simple screening models (Level 1) are utilised first before the application of more advanced models (Level 2 & 3).

For this Baseline Modelling Assessment study, a detailed understanding of the air quality impacts (time and space variation of the concentrations) is required. Additionally this modelling study must be able to account for: causality effects, calms, non-linear plume trajectories, spatial variations in turbulent mixing, multiple source types and chemical transformations. Thus in light of the above, a Level 3 modelling assessment was conducted for this study.

3.3 MODELS UTILISED IN STUDY

3.3.1 METEOROLOGICAL MODEL

Air quality is strongly influenced by meteorology which covers an array of atmospheric processes that determines the evolution of emissions, chemical species, aerosols and particulate matter (Seaman, 2000). Thus the performance of atmospheric dispersion models depends critically on the meteorological data to simulate the fate and transport of air pollution (Busillo et al., 2005; Davakis et al., 2007; Pielke and Uliasz, 1998). The representativeness of meteorological data is a key factor in accurately modelling the dispersion of these pollutants since meteorological conditions are not uniform over larger distances or in complex terrain, coastal environments, or in urban areas (Alapaty., 1994; Moschandreas et al., 2002).

South Africa is constrained by the lack of an adequate network of surface and upper air meteorological stations that are representative of the atmospheric boundary layer near the surface or at higher levels (Zunckel, 2007). Further, spatially and temporally representative wind flow statistics are not widely available for South Africa (Raghunandan et al., 2008). For this study, no upper air meteorological data are recorded within the modelling domain and the nearest upper air station is located at Irene in Pretoria. Therefore due to the scarcity of surface and upper air meteorological stations available for the study area, *TAPM* was used to provide site-specific and representative meteorological data to drive the dispersion model.

TAPM

TAPM, developed by the Australian CSIRO Atmospheric Research Division, is an integrated 3-dimensional mesoscale prognostic meteorological and air pollution regulatory model that is controlled by a graphical user interface (Hurley et al, 2005a; Hurley, 2005b; Luhar and Hurley, 2004; Zawar-Reza et al., 2005).

The meteorological component of TAPM is an incompressible, optionally non-hydrostatic, primitive equation model which uses a terrain-following vertical coordinate system for 3-dimensional simulations (Zawar-Reza and Sturman, 2008). It includes comprehensive parameterisations for cloud/rain micro-physical processes, urban/vegetative canopy and soil, turbulence closure and radiative fluxes (Katzfey and Ryan, 1997; Lai and Chang, 2009; Mahrer and Pielke, 1977)

TAPM predicts local-scale flows, for instance sea breezes and terrain-induced circulations, by utilising meteorological fields obtained from larger scale synoptic analyses (Luhar and Hurley, 2004).

TAPM is able to make use of fundamental fluid dynamics and scalar transport equations to predict the underlying meteorology of an area (Hurley, 2005c). It solves the momentum equations to determine the mean horizontal wind components, the incompressible continuity equation for vertical velocity, and scalar equations for potential virtual temperature and moisture (Luhar and Hurley, 2004). The model allows for the option of observed wind data to be assimilated into the momentum equations as nudging terms (Luhar and Hurley, 2003; Raghunandan et al., 2008). Potential virtual temperature is determined from an equation combining the conservation of heat and water vapour. Pressure is determined by the application of a Poisson equation to the nonhydrostatic component (Luhar and Hurley, 2003; Hurley 2005b). A detailed description of the equations and parameterisations, including the numerical methods used to solve the model equations, used in the present study is given by Hurley et al. (2005a) and Hurley (2005c).

TAPM uses databases of global terrain height, land use, sea-surface temperature and synoptic meteorological analyses as input. The global terrain height and land use datasets are available at a grid space resolution of approximately 1 km whilst the sea surface temperature and synoptic scale meteorological datasets are available at 100 km resolution. The global terrain height and land use datasets are sourced from the US Geological Survey (USGS), Earth Resources Observation Systems (EROS) and the Data Center Distributed Active Archive Center (EDC DAAC) data (Hurley, 2005b). The global long-term monthly mean sea surface temperatures are derived from the US National Center for Atmospheric Research and the synoptic scale analyses are obtained from the Australian Bureau of Meteorology.

3.3.2 Dispersion Model

For this Level 3 tier modelling assessment, the US-EPA approved Californian Puff (CALPUFF) modelling suite was utilised.

CALPUFF Modelling Suite

For The California Puff (CALPUFF) model is an integrated modelling system which can simulate the effects of time- and space-varying meteorological conditions for pollutant dispersion, transformation and deposition (USEPA, 2005; Zhou et al., 2006). The CALPUFF modelling suite comprises of three main components: CALMET, CALPUFF and CALPOST (Figure 21). CALMET is the diagnostic meteorological model that develops hourly surface wind structures and micrometeorological variables on a three-dimensional gridded domain for CALPUFF (Elbir, 2006; Hao et al., 2007; Lopez et al., 2005; Song et al., 2006; Zhou et al., 2003). CALPUFF is a non-steady-state Gaussian based

transport and dispersion model. It uses the three-dimensional meteorological fields developed by CALMET and a series of overlapping puffs to represent the spatial and temporal distribution of emissions from a source (Scire et al., 2000b; Song et al., 2006). CALPOST is then used as a postprocessor for the CALPUFF outputs to produce a tabulated summary of the simulation results (Wang, 2006). A brief overview of the CALMET and CALPUFF models is presented here.

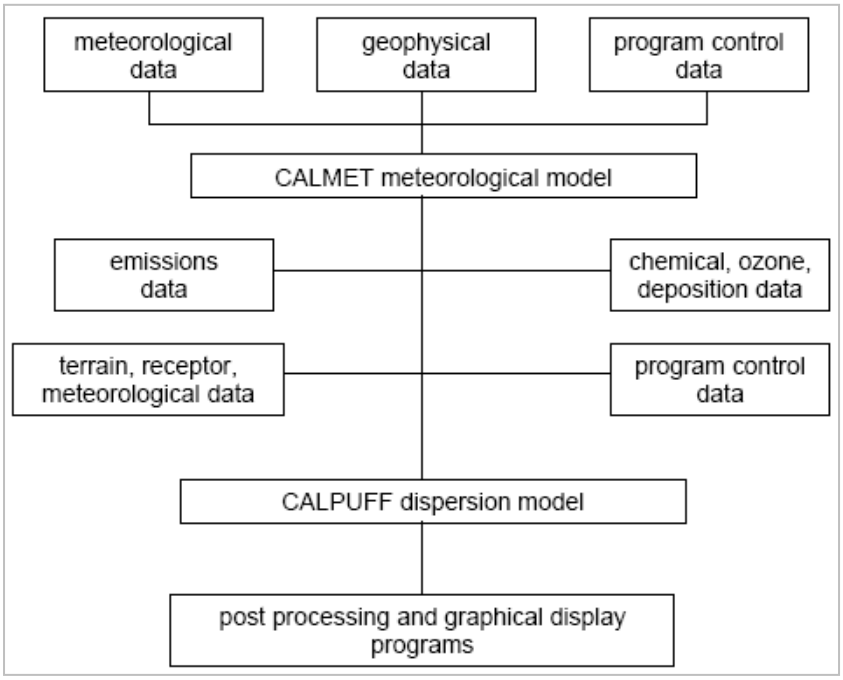

Figure 20: CALPUFF modelling system (Source: SRC, 2008)

CALMET

A three-dimensional wind field is computed by the CALMET meteorological model (USEPA, 2005). CALMET requires both geophysical data (terrain elevations and land use categories) and hourly meteorological data (wind speed, wind direction, temperature, cloud cover, ceiling height, surface pressure, relative humidity, precipitation and upper air sounding data) (USEPA, 2005; Scire and Robe, 2004).

CALMET consists of an advanced diagnostic wind field generator as well as a micrometeorological module for overwater and overland boundary layers. An initial guess wind field is modified to take account of kinematic effects of terrain, slope flows, valley flows and terrain blocking effects to create a Step 1 wind field. Observational data are then combined with this Step 1 wind field through an objective analysis procedure to generate the final Step 2 wind field (USEPA 2005; Scire 1999a; Scire 2000a). CALPUFF advects and disperses along these wind vectors created by CALMET (Allwine et al., 1998).

CALPUFF

CALPUFF is a non-steady-state, time-and space-dependent Gaussian puff model which is designed to simulate the transport, dispersion, chemical reactions and deposition of gases and particles in the atmosphere (Ainslie and Jackson, 2009; Scire et al., 2000b). CALPUFF treats emissions as a series of continuous puffs. Each puff is allowed to move with the ambient wind flow (Moschandreas et al, 2006). As the wind flow changes from hour to hour, the path of each puff is displaced in a Lagrangian fashion while undergoing Gaussian dispersion. The model predicted concentrations are calculated based on the contributions of each puff as it passes near or over a discrete receptor point in the modelling domain (Scire et al., 2000b).

CALPUFF is able to model four different source types: point, line, volume and area sources for a single modelling domain. The model makes use of similarity theory to estimate the horizontal and vertical plume dispersion coefficients and contains comprehensive algorithms for both near-source stack and building effects (such as building downwash, partial penetration, plume rise) and longer-range effects (chemical transformation, deposition, plume fumigation) (Ainslie and Jackson, 2009; Holmes and Morawska, 2006; USEPA, 2005).

The non-steady state approach of the CALPUFF model makes use of a full three-dimensional meteorological field which can account for spatial and temporal variability in the wind field and atmospheric stability (Scire and Robe, 2004). Thus CALPUFF is able to take account of complex terrain effects, wind reversals, wind stagnation, and causality effects over large spatial scales (Beychok, 2005; Hao et al., 2007; Paradiz et al., 2008). These provide a more realistic simulation of reality for dispersion and transport as opposed to steady-state Gaussian plume models (Elbir, 2003 Moschandreas et al, 2006).

3.4 EMISSIONS INVENTORY UTILISED IN MODELLING

The identification of existing sources of emission in the region and the characterisation of existing ambient pollutant concentrations is fundamental to the assessment of the potential for cumulative impacts and synergistic effects given the existing operations and their associated emissions. Thus in order to identify possible effects of reduction measures in an area it is necessary to prepare a representative emission source inventory. An emissions inventory was compiled for the modelling domain (Figure 30) which included the source catergories for: power generation; residential, vehicle and biomass emissions.

3.4.1 POWER GENERATION SOURCES

It's only the Eskom Majuba Power Station (4 110 MW) (Figure 21) that is located within the study domain (Figure 30). The emissions inventory was based on Eskom"s reported emissions for the period 2017 to 2019. The emissions inventory is shown in Table 4 & 5 below.

Table 4: Model efflux parameters for Eskom Majuba Power Station

Source	Diameter (m)	Height (m)	Exit Temp (K)	Exit Velocity (m/s)	SO_2 (t/a)	NO_2 (t/a)	PM_{10}	$PM_{2.5}$
Majuba	12.3	250	398	22	81 896	69 825	1403	1198
	12.3	250	398	22	81 896	69 825	1403	1198

Table 5: Eskom Coal Stockpile

	PM_{10} (t/a)	$PM_{2.5}$ (t/a)
COAL STOCKPILE	**COAL STOCKPILE**	**COAL STOCKPILE**
Materials Handling (quantity-based)	1.4	0.2
Wind Erosion (surface area-based)	49.5	19.8
Sub total	**50.9**	**20.0**
ASH DUMP	**ASH DUMP**	**ASH DUMP**
Materials Handling (quantity-based)	0.1	0.0
Wind Erosion (surface area-based)	540.6	216.3
Sub total	**540.7**	**216.3**
TOTAL	**591.6**	**236.3**

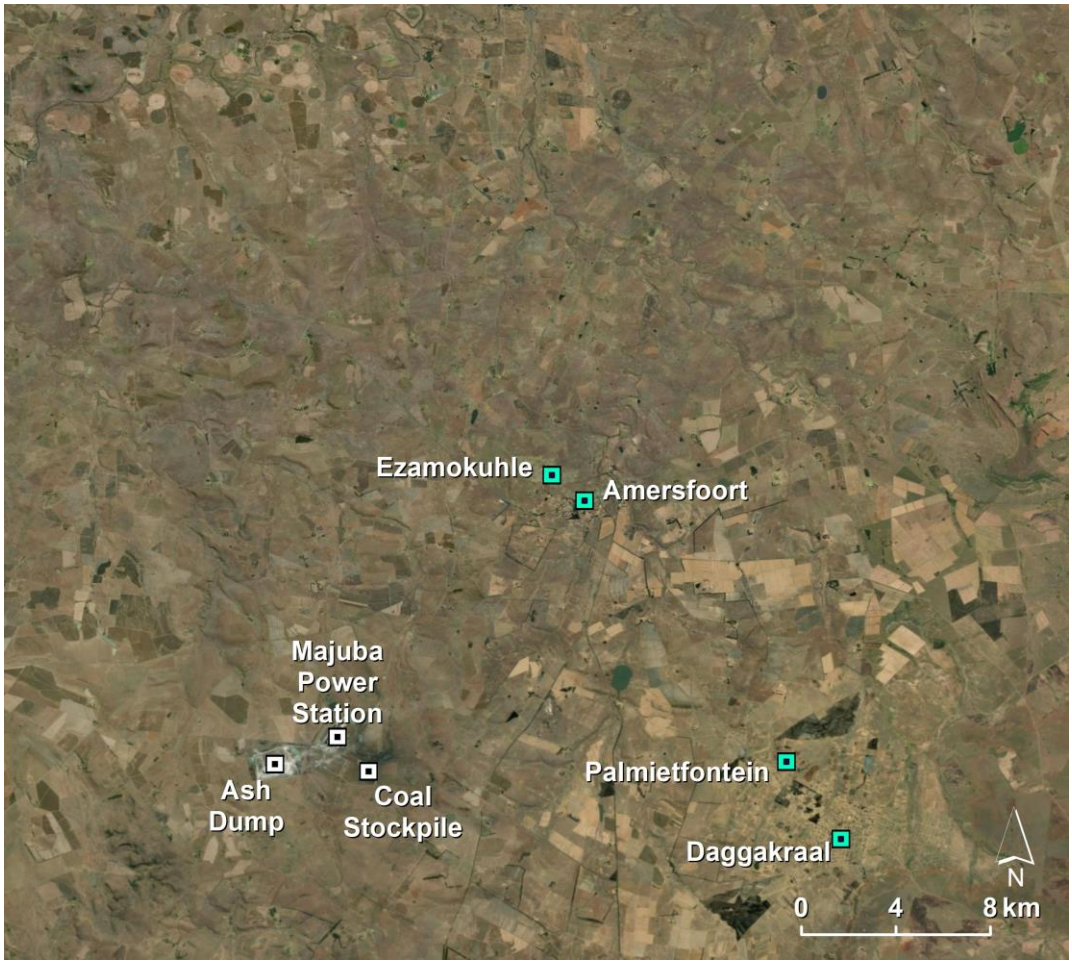

Figure 21: Map showing the location of Majuba Power Station & Coal Stockpile

3.4.2 VEHICLE EMISSIONS

Emissions from vehicles arise during the different cycles of driving from start-up, during driving, evaporation from the engine and fuel line, and during re-fueling (DEFF, 2010). Particulate matter is also emitted from brake, tyre and road wear (DEFF, 2013). Other pollutants associated with vehicle emissions include SO_2, NO_x, CO, C_6H_6 and P_b. The emission rates are co-dependent on various factors relating to vehicle *parc* (vehicle class, model, speed and maintenance); fuel specifications and environmental factors (Samaras *et al*., 1999). Vehicular emissions for all municipalities in South Africa were calculated in the *Integrated Strategy for the Control of Motor Vehicle Emissions* (DEFF, 2013). The vehicle categories herein included passenger cars, light duty vehicles, heavy duty vehicles, buses and motorcycles. To calculate the emissions, a top-down approach was utilised wherein Tier 1 emission factors developed by the European Environmental Agency (Table 6 to 8)

were applied to fuel sales data. The estimated emissions (Table 9) for the Pixley ka Seme Local Municipality was utilised in the baseline modelling assessment (Figure 22).

Table 6: Tier 1 emission factors for combustion from motor vehicle emissions (DEFF, 2013)

Category	Fuel	Emission Factor (g/kg Fuel)						
		NO_x	SO_2	CO	PM_{10}	NMVOC	Lead	CO_2 [1]
Motorcycles	Gasoline	9.50	-	490	2.7	114	0.00007	69 300
Passenger cars	Gasoline	14.5	-	132	0.037	14	0.000017	69 300
	Diesel 50	11	0.1	4.7	1.7	1.1	0.0000325	74 100
Light-duty vehicles	Gasoline	24	-	155	0.03	14	0.000017	69 300
	Diesel 500	11	1	4.7	1.7	1.1	0.0000325	74 100
Heavy-duty vehicles and buses	Diesel 500	37	1	8	1.2	1.6	0.0000325	74 100

Notes: CO_2 emission factor unit is kg/TJ (IPCC, 2006)

Table 7: Tier 1 PM_{10} emission factors for tyre and brake wear and road surface wear (DEFF, 2013)

Category	Emission Factor (g/km/vehicle)
Motorcycles	0.0064
Passenger cars	0.0138
Light-duty vehicles	0.0216
Heavy-duty vehicles and buses	0.0590

Table 8: Tier 1 emission factors for evaporation from motor vehicle emissions (DEFF, 2013)

Category	Fuel	Emission Factor (g/vehicle/day)	
		NMVOC	Benzene
Motorcycles	Gasoline	3	0.0291
Passenger cars	Gasoline	14.8	0.14356
	Diesel 50	-	-
Light-duty vehicles	Gasoline	2.6	0.21922
	Diesel 500	--	-
Heavy-duty vehicles and buses	Diesel 500	-	-

Table 9: Pixley ka Seme Local Municipality vehicle emissions in tons/yr (DEFF, 2013)

NO_x	SO_2	CO	PM_{10}	NMVOC	Benzene	Lead	CO_2
355	6.9	1 797	12.7	238	0.31	0.00045	59 595

Figure 22: Major roads utilised in the simulation

3.4.3 Residential Fuel Burning

Residential fuel burning for the modelling was estimated based on energy use data at the sub-place level for: Ezamokuhle (Figure 23) and Daggakraal including Vlakplaats & Vlakpoort (Figure 24) obtained from the 2011 Census (StatsSA, 2011). The 2011 Census delineates the number of households utilising fuels for domestic purposes (cooking, lighting, space heating) as shown in Tables 10 and 11.

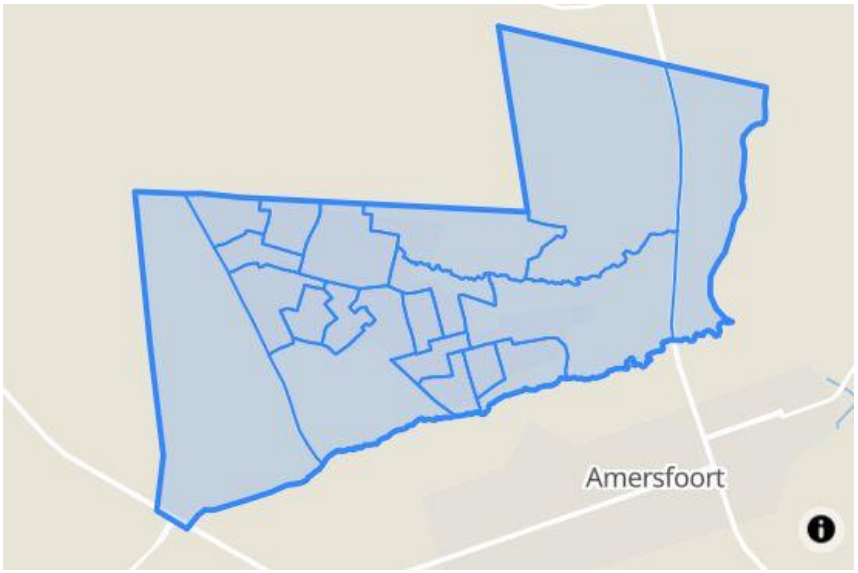

Figure 23: Map of Ezamokuhle at the sub-place level (Stats SA, 2011)

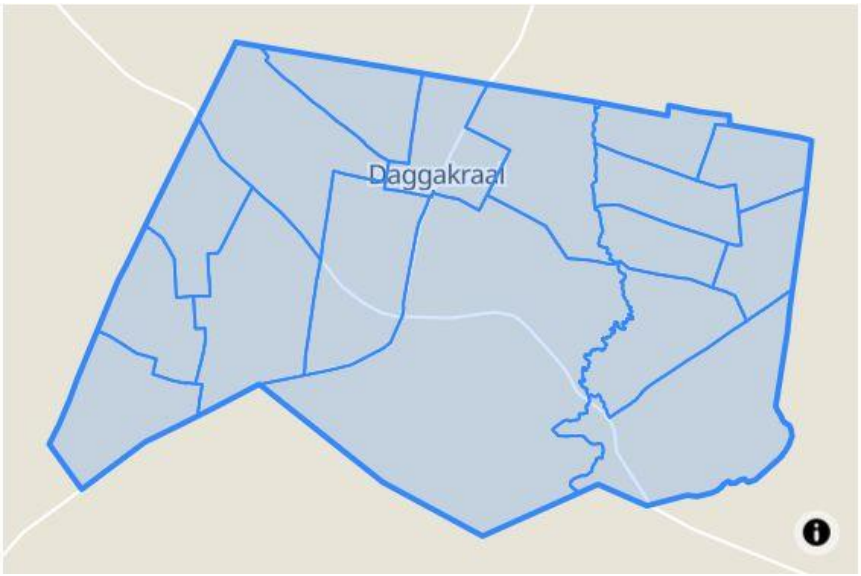

Figure 24: Map of Daggakraal at the sub-place level (Stats SA, 2011)

It's evident from Table 10 & 11 that overall, electricity is the preferred energy source throughout the households in Ezamokuhle. Coal is also a popular energy option for the Ezamokuhle of homes.

Table 10: Residential fuel usage (% of households) within Ezamokhule

Energy Source	Cooking	Heating	Lightning
Electricity	71.1	53.4	53.4
Gas	0.4	0.5	0.5
Paraffin	3.3	1.3	1.3
Solar	0.1	0.2	32.4
Candles	0	0	0.9
Wood	0.9	0.9	0
Coal	22.8	32.4	0
Animal Dung	0.6	0.8	0
Other	0.1	0	0
None	0.7	10.5	0.8

Table 11: Residential fuel usage (% of households) within Daggakraal

Energy Source	Cooking	Heating	Lightning
Electricity	29.3	18	18
Gas	0.4	0.4	0.4
Paraffin	1.5	0.8	0.8
Solar	0	0	65.8
Candles	0	0	5.2
Wood	3.5	5.2	0
Coal	60	65.8	0
Animal Dung	5	6.4	0
Other	0	0	0
None	0.4	3.4	6.4

The total quantities of fuels being consumed by the households at a sub-place level were estimated based on the typical monthly fuel use figures, given by Afrane-Okese (1999). The DEFF emission factors for residential fuel burning (DEFF, 2019) were then applied to calculate the resultant emissions for the study (Table 13).

Table 12: Emission factors for Residential Fuel Burning (DEFF, 2019)

Fuel Type	Emission Factor					
	PM_{10}	$PM_{2.5}$	SO_2	NO_x	CO	VOC
Coal(g/kg)	16.146	16.146	11.6	3.95	94.38	5
Paraffin(g/l)	0.359	0.359	0.851	1.5	44.9	0.085
Wood(g/Kg)	13.745	13.745	0.123	1.224	114.577	19.867
Gas(g/kg)	0.068	0.068	0.01	1.4	13.6	0.018

Table 13: Estimated residential fuel burning emissions in tons per year for the study area

	Emission rate (tons per annum)			
	SO_2	NO_x	PM_{10}	$PM_{2.5}$
Amersfoort	0.44	0.07	0.06	0.04
Ezamokuhle	2.0	0.3	0.3	0.2
Majuba	0.0037	0.0009	0.0004	0.0002
Palmietfontein	0.5	0.1	0.1	0.1
Daggakraal	6.2	1.0	1.1	0.8

The location of the residential fuel burning sources (burning coal, wood, and/or paraffin) is shown in Figure 25.

Figure 25: Location of residential fuel burning areas indicated by black outlines utilized in the Study

3.4.4 Biomass Burning

Biomass burning refers to the large scale burning of vegetation, which includes savanna, forests and grasslands, domestic fuels and agricultural wastes (Andreae, 1991; Crutzen and Andreae, 1990).

Fires emit large volumes of PM, CO, NOx and VOC (DEFF, 2012). Biomass burning occurs predominantly during the dry season corresponding to the period from May to October in southern Africa (Cahoon et al., 1996; Scholes et al., 1996a, 1996b; Scholes and Andreae, 2000; Swap et al., 1996).

The majority of fires on the Highveld are thought to be anthropogenic and include veld fires, burning of grazing land and crop-residue (DEFF, 2010). The biomes (Figure 26) which are categorised as high to extreme risk include the following: fynbos, savanna and grassland. Mpumalanga is predominantly a grassland biome thus an area at high to extreme risk of veld fires.

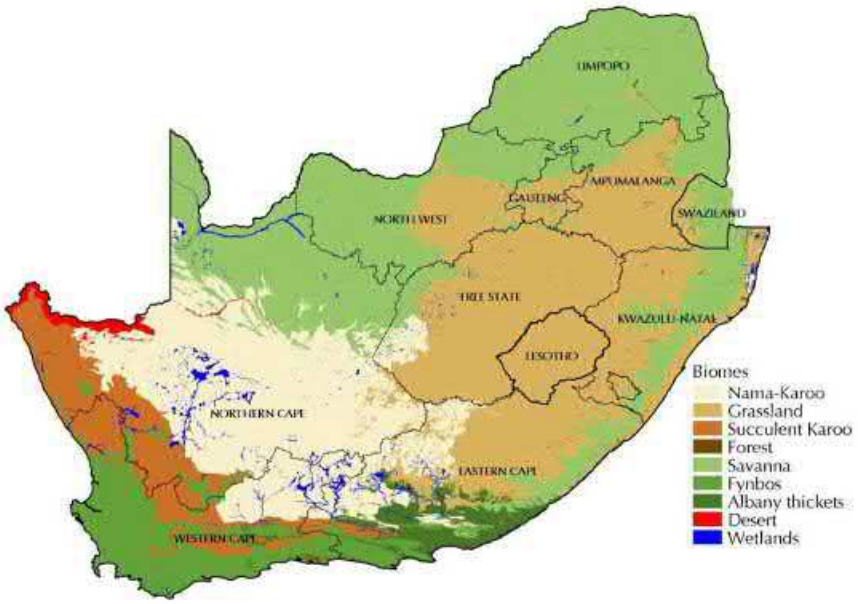

Figure 26: South African Biomes (SANBI, 2004)

According to DEFF (2010) the emission of criteria pollutants from biomass fires is calculated by the general formula:

Emission = (Area burned) x (Fuel Load) x (Completeness of combustion) x (Emission Factor)

The total area burned annually was based on remote sensing data from the CSIR's Meraka Institute. The fuel load was estimated using the vegetation map (SANBI, 2006). For fuel combustion completeness factors, the IPCC GHG Inventory Guideline 2006 (IPCC 2006) was adapted using the soil fertility classes from the South African National Land Cover map. The emission factors were

based on Safari 2000 data (Ito and Penner, 2004). The biomass emissions utilized in the study is shown in Table 14 and shown in Figure 27.

Table 14: Estimated biomass burning emissions

Emission rate (tons per annum)			
SO_2	NO_x	PM_{10}	$PM_{2.5}$
5.2	58.4	149.8	80.9

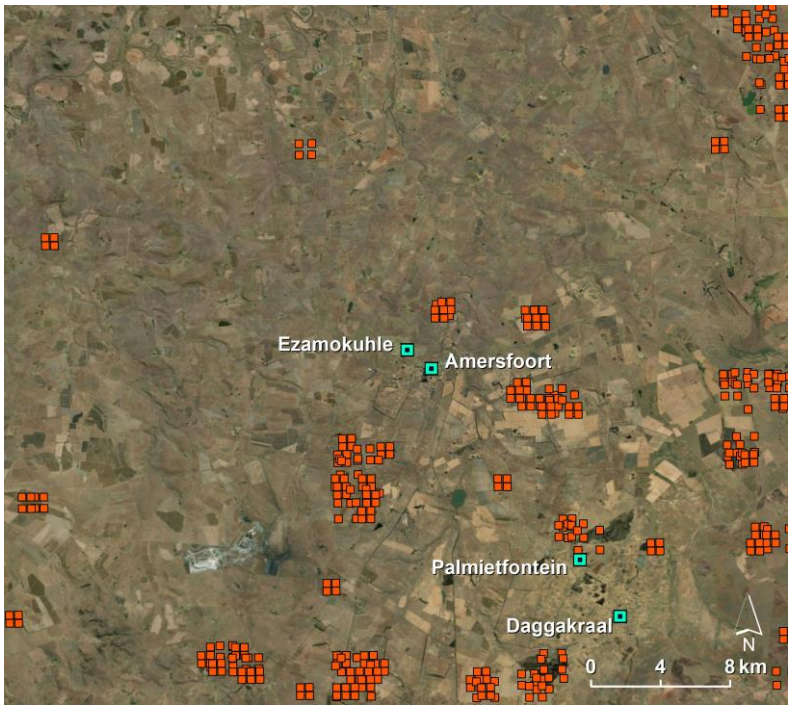

Figure 27: Location of biomass burning emissions indicated by orange polygons utilized in the Study

An overview of all emission source catergories utilized in the simulation is provided in Figure 28.

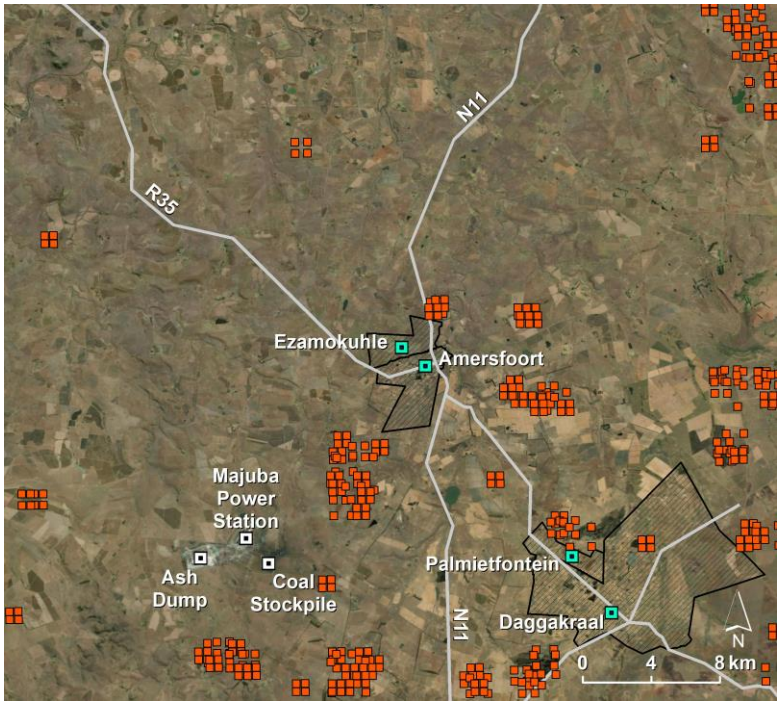

Figure 28: Overview of all emission source catergories utilized in the Study

3.5 Emissions scenarios and Pollutants simulated

3.5.1 Emission Scenarios

The baseline modelling assessment was simulated utilising the emissions inventory outlined in section 3.4 to assess the air quality impact in Ezamokuhle.

3.5.2 Pollutants

The CALPUFF modelling suite was utilised to predict the dispersion of the following pollutants: SO_2; SO_4^{2-}; NO_2; NO_3, PM_{10} and $PM_{2.5}$. The dispersion of the pollutants were simulated for the prevailing meteorological conditions for the period 1 January 2017 to 31 December 2019 for each modelling domain.

- *3.5.2.1 Total Particulate Calculation*

Ambient particulate matter is a complex mixture of inorganic and organic compounds. The NAAQS (Table 1) regulates particulate matter for different size fractions (PM_{10} and $PM_{2.5}$) which are based on epidemiological evidence for mortality and cardiorespiratory health effects.

Sulphate and nitrate constitute a significant portion of the particle mass in the atmosphere. According to Reis *et. al* (2007) few epidemiological studies have included the sulfate content of particulate matter as a specific variable in health effect analyses. There is considerably less data for nitrates.

Reis *et. al* (2007) however demonstrated epidemiologic and toxicological evidence provide little or no support for a causal association of particulate sulfate and health risk at ambient concentrations. Further for nitrate-containing particulate matter, there is no epidemiological data and the toxicological evidence does not support a causal association between particulate nitrate compounds and excess health risks. There is insufficient evidence to include or exclude secondary organic processes for sulphates & nitrates as being potentially important to particulate matter associated health risk. (Reis *et. al*, 2007).

This baseline modelling study has taken a conservative approach (Scire, 2014) whereby the total concentrations of particulate matter (PM_{10} or $PM_{2.5}$) was computed as the sum of primary particulate matter concentrations (PM_{10} or $PM_{2.5}$) plus the contribution of concentrations from secondary particulate matter, including ammonium nitrate and ammonium sulfate as shown below:

Total PM_{10} or $PM_{2.5}$ = sum of (PM_{10} or $PM_{2.5}$) + $(NH_4)_2SO_4$ + NH_4NO_3

This total concentrations of particulate matter (either PM_{10} or $PM_{2.5}$) was then compared to the applicable PM_{10} or $PM_{2.5}$ NAAQS limit (Table 1).

3.6 Modelling Grids & Receptors

3.6.1 Meteological Model Grids

- *TAPM*

TAPM was used to model the hourly surface and upper air meteorology for the study area, for the period 2017 to 2019. TAPM was initially run for a larger mother domain meteorological grid which was then used to initialise the smaller fine-resolution modelling grids. The outer domain is 600 km by 600 km at a 24 km grid resolution, the middle domain is 300 km by 300 km at a 12 km grid resolution and the inner domain is 75 km by 75 km at a 3 km grid resolution (Figure 29). These simulations used as model input the default databases of global terrain height data, land use and synoptic scale meteorological analyses data as discussed previously (section 3.3).

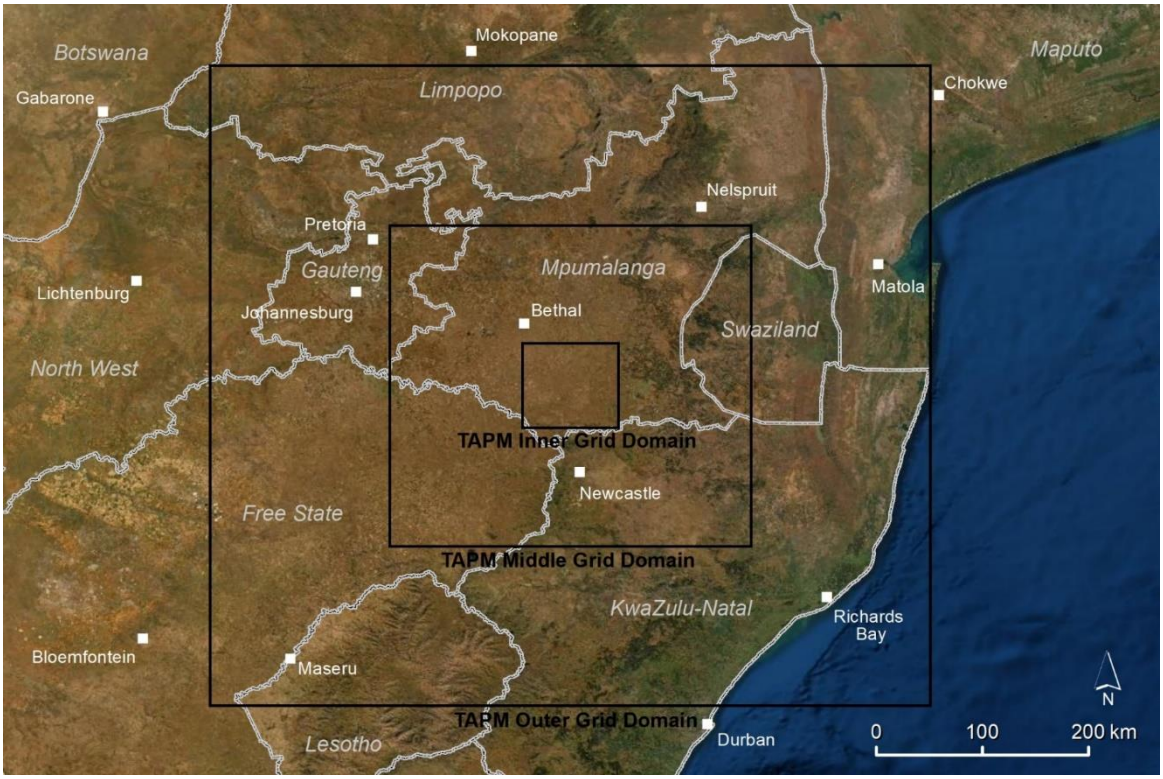

Figure 29: Nested grid domains used in the TAPM simulation

- *CALMET*

The CALMET modelling domain for the study area has an extent of 65 km by 65 km with a uniformly spaced horizontal grid resolution of 0.5 km. The top of the domain was set at 5 km with 12 vertical levels (Figure 30).

3.6.2 Dispersion Modelling Grids

- *CALPUFF*

A primary (coarse resolution) grid and a secondary grid (finer resolution) was utilised in the CALPUFF simulations (Figure 30). The grid specifications for each modelling domain is specified in Table 15.

Table 15: Modelling domain grid specifications

Variable	Primary Grid	Secondary Grid
Spatial Area (km^2)	1600	36
Grid Distance (km) in x and y direction	40 x 40	6 x 6
Horizontal Grid resolution (m)	500	200
Number of grid cells in x and y direction	80 x 80	30 x 30
Total number of gridded receptors in domain	6400	900

PRIMARY MODELLING GRID

The domain extends 40 km (west-east) by 40 km (north-south) for a CALPUFF modelling domain of 1600 km^2. It consists of a uniformly spaced Cartesian receptor grid with 500 m spacing, giving 6400 grid cells (80x80 grid cells). This modelling domain accounts for a range of emission sources within a 20 km radius around Ezamokuhle.

SECONDARY MODELLING GRID

The domain extends 8 km (west-east) by 8 km (north-south) for a CALPUFF modelling domain of 36 km^2. It will consist of a uniformly spaced Cartesian receptor grid with 200 m spacing, giving 1600 grid cells (40x40 grid cells). This fine grid resolution ensures that dispersion characteristics and ambient concentrations are accurately captured within and in the immediate vicinity of Ezamokuhle.

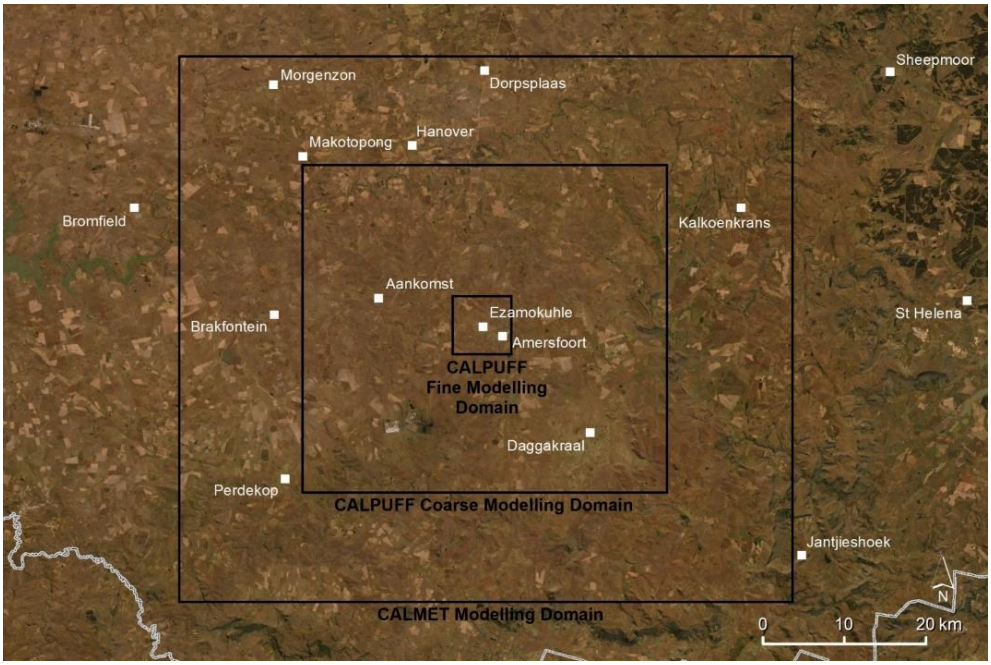

Figure 30: CALPUFF Modelling Domains

3.6.3 RECEPTOR

The location of the discrete receptors that were selected in the modelling domains are illustrated in Figures 31 and 32.

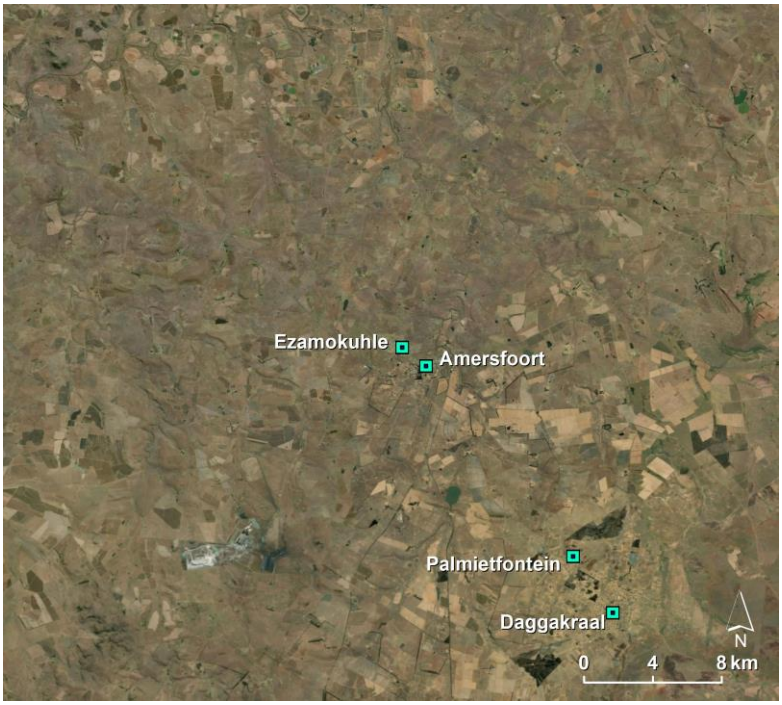

Figure 31: Location of discrete receptors in the primary modelling domain

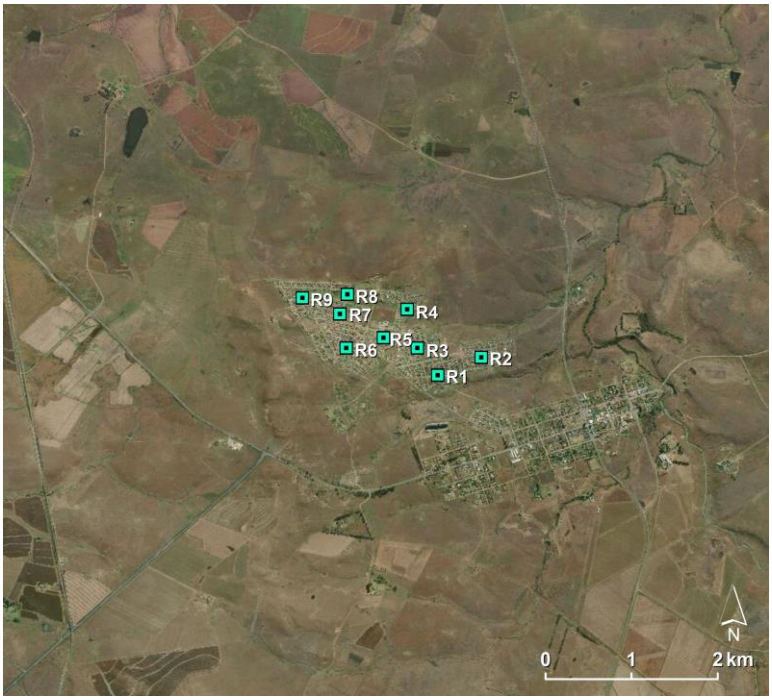

Figure 32: Location of discrete receptors (R1 to R9) in the secondary modelling domain

3.7 Model Settings

A summary of the model control options for CALMET and CALPUFF is provided in Tables 16 & 17.

Table 16: Parameterization of key variables for CALMET

Parameter	Model value
12 vertical cell face heights (m)	0, 20, 40, 80, 160, 320, 640, 1000, 1500, 2000, 2500, 3000, 4000
Coriolis parameter (per second)	0.0001
Empirical constants for mixing height equation	Neutral, mechanical: 1.41 Convective: 0.15 Stable: 2400 Overwater, mechanical: 0.12
Minimum potential temperature lapse rate (K/m)	0.001
Depth of layer above convective mixing height through which lapse rate is computed (m)	200
Wind field model	Diagnostic wind module
Surface wind extrapolation	Similarity theory
Restrictions on extrapolation of surface data	No extrapolation as modelled upper air data field is applied
Radius of influence of terrain features (km)	5
Radius of influence of surface stations (km)	No used as continuous surface data field is applied

Table 17: Parameterization of key variables for CALPUFF

Parameter	Model value
Chemical transformation	Default NO_2 conversion factor is applied
Wind speed profile	Rural
Calm conditions	Wind speed < 0.5 m/s
Plume rise	Transitional plume rise, stack tip downwash, and partial plume penetration is modelled
Dispersion	CALPUFF used in PUFF mode

Dispersion option	Pasquill-Gifford coefficients are used for rural and McElroy-Pooler coefficients are used for urban
Terrain adjustment method	Partial plume path adjustment

RESULTS & DISCUSSION

The CALPUFF modelling suite was utilised to predict the dispersion of the following pollutants: SO_2; SO_4^{2-}; NO_2; NO_3, PM_{10} and $PM_{2.5}$. The total concentrations of particulate matter (PM_{10} or $PM_{2.5}$) were computed as the sum of primary particulate matter concentrations (PM_{10} or $PM_{2.5}$) plus the contribution of concentrations from secondary particulate matter, including ammonium nitrate and ammonium sulfate (section 3.5.2.1).

The modelled 99th percentile hourly and daily as well as the annual average modelled concentrations for SO_2, NO_2 and PM_{10} for sensitive receptors (section 3.6.3) were assessed against the NAAQS (Table 1). The dispersion of the pollutants were simulated for the prevailing meteorological conditions for the period 1 January 2017 to 31 December 2019 for each modelling domain (section 3.6.2).

Section 4.1 assess the predicted ambient concentrations against the NAAQS compliance limits (Table 1) for SO_2, NO_2, PM_{10} and $PM_{2.5}$ for the primary modelling domain. Whilst section 4.2 utilising the model predicted results identifies “hotspot zones” to inform the appropriate & representative placement of the ambient air quality analysers at Ezamokuhle.

4.1 Model Predicted Concentrations to NAAQS

4.1.1 SO_2

The model predicted 99th percentile hourly, daily and annual average ambient SO2 concentrations as a result of all SO_2 emissions sources are generally in compliance with the NAAQS (Tables 18 to 20) in the modelling domain (Figures 36 to 38). Ambient air quality concentrations of SO_2 for each discrete receptor is illustrated by Figures 33 to 35. The trend analysis and polar plots (Figure 11 and 17) shows that peak SO_2 concentrations are present at high wind speeds thus indicative of emissions from stacks rather than non-buoyant ground-level sources. Hence the higher SO_2 concentrations associated with the south-westerly winds are most likely due to emissions from the Eskom Majuba station (Figure 17). Further elevated winter concentration of SO_2 indicate the contribution of residential fuel burning to the ambient SO_2 concentrations (Figure 11).

Table 18: Hourly SO_2 99th percentile modelled concentrations (µg/m^3) calculated at the discrete receptors for the period 2017 to 2019

Receptor	NAAQS	Model Predicted Hourly SO_2 Concentration
Ezamokuhle	350	114
Amersfoort		115
Daggakraal		121
Palmietfontein		135

Table 19: Daily SO_2 99th percentile modelled concentrations (µg/m^3) calculated at the discrete receptors for the period 2017 to 2019

Receptor	NAAQS	Model Predicted Daily SO_2 Concentration
Ezamokuhle	125	54
Amersfoort		47
Daggakraal		39
Palmietfontein		43

Table 20: Annual SO_2 modelled concentration (µg/m3) calculated at the discrete receptors for the period 2017 to 2019

Receptor	NAAQS	Model Predicted Annual SO_2 Concentration
Ezamokuhle	50	6
Amersfoort		4
Daggakraal		6
Palmietfontein		7

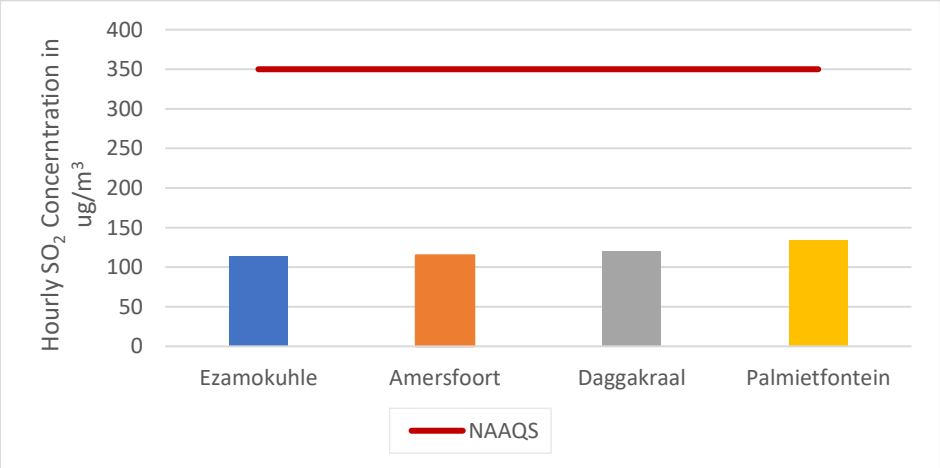

Figure 33: Hourly SO_2 99th percentile modelled concentrations (µg/m3) calculated at the discrete receptors for the period 2017 to 2019

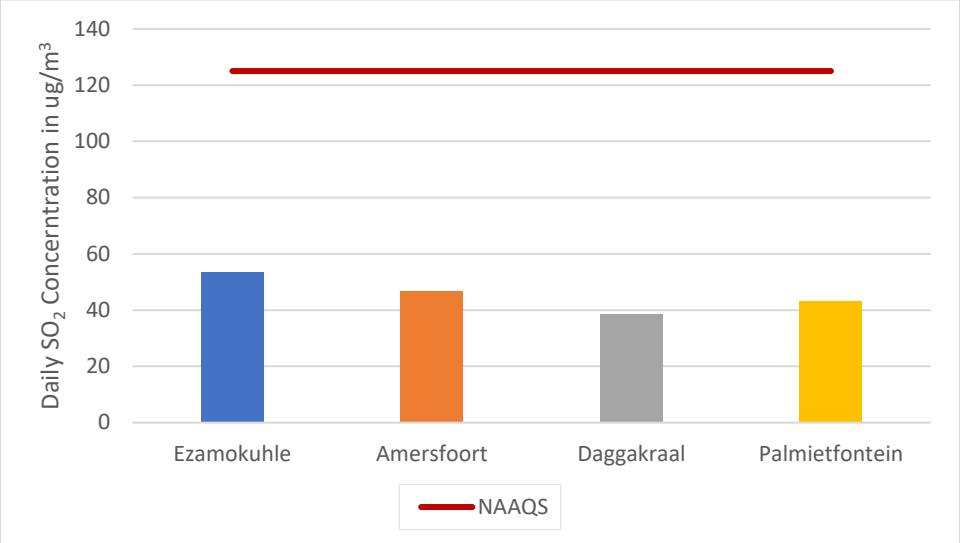

Figure 34: Daily SO_2 99th percentile modelled concentrations (µg/m3) calculated at the discrete receptors for the period 2017 to 2019

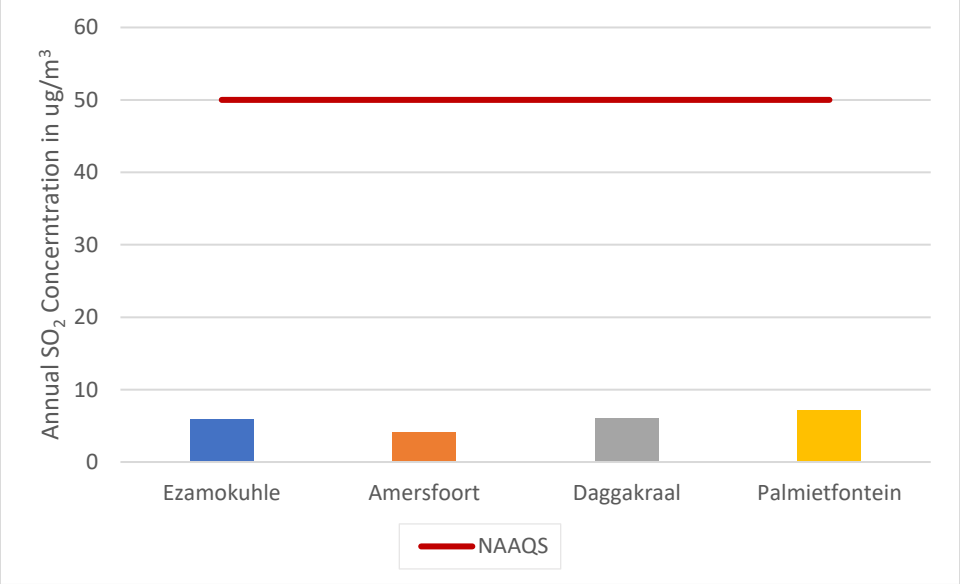

Figure 35: Annual SO_2 modelled concentration (µg/m3) calculated at the discrete receptors for the period 2017 to 2019

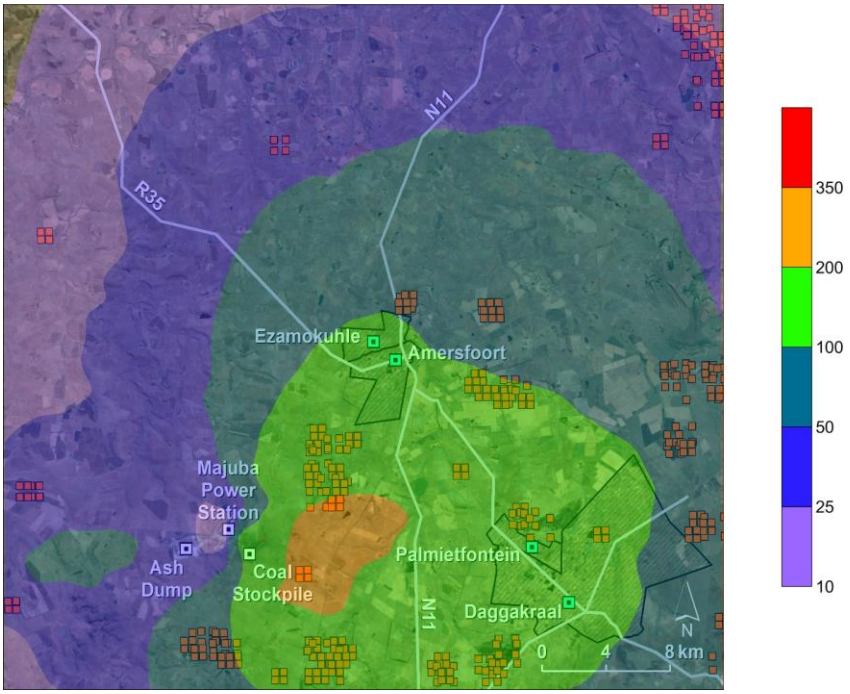

Figure 36: Model predicted 99th percentile houry SO_2 ambient air quality concentration in µg/m³

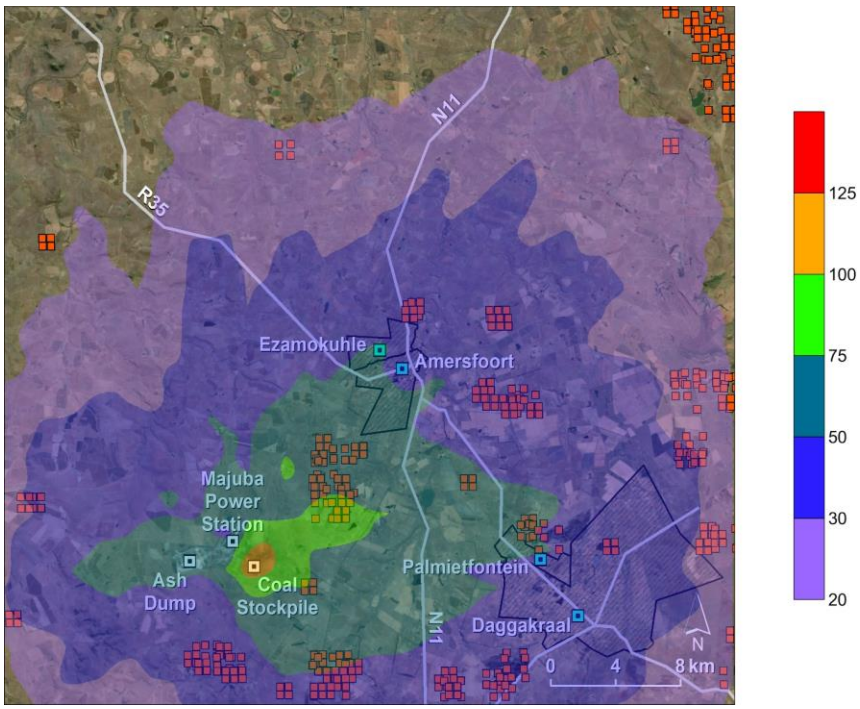

Figure 37: Model predicted 99th percentile houry SO_2 ambient air quality concentration in µg/m³

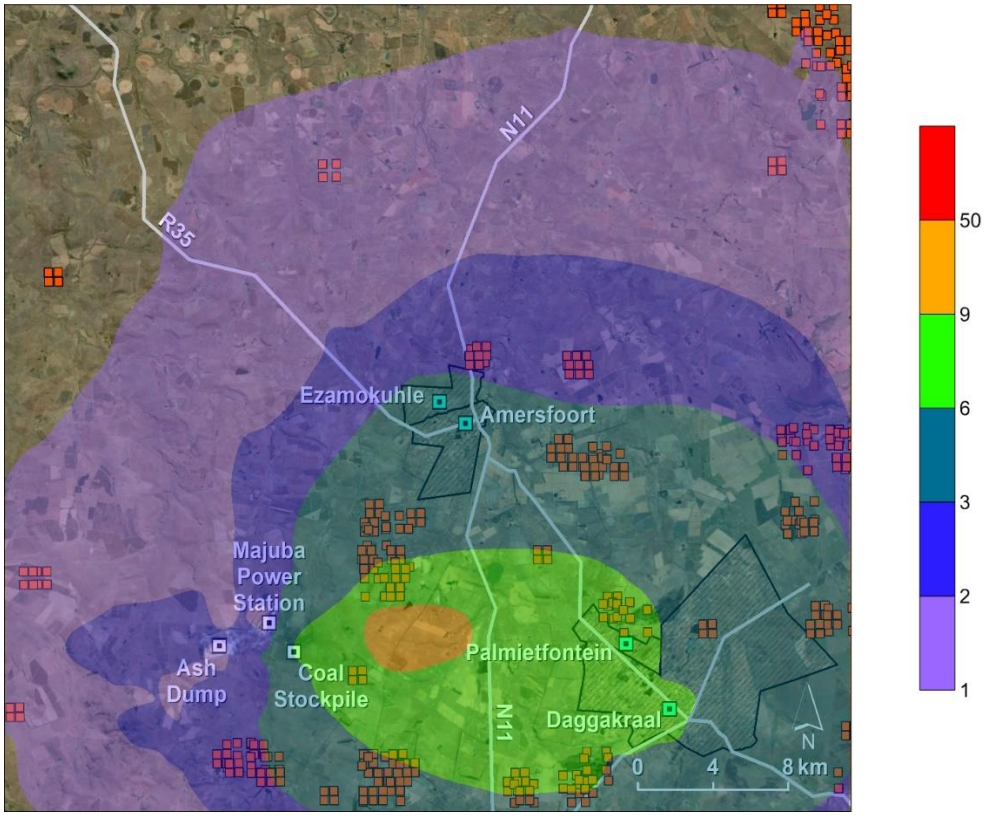

Figure 38: Model predicted annualSO_2 ambient air quality concentration in µg/m^3

4.1.2 NO_2

The model predicted 99th percentile hourly and annual ambient NO_2 concentrations as a result of all NO_2 emissions sources utilised in this study are in compliance with the NAAQS (Tables 21 & 22) at all discrete receptors (Figures 39 to 42). At the Eskom Ezamokuhle station (Figure 11), the high NO_2 concentrations occur under stable atmospheric conditions when non-buoyant ground-level sources are important. The time variation plot at Ezamokuhle explicitly reveals that the variability of NO_2 concentrations are conditioned by vehicle emissions. Additionally the polar plot indicates the impact of NO_2 levels in winter at the Eskom Ezamokuhle and Majuba stations demonstrate the additional contribution of residential fuel burning sources.

Table 21: Hourly NO_2 99th percentile modelled concentrations (µg/m^3) calculated at the discrete receptors for the period 2017 to 2019

Receptor	NAAQS	Model Predicted Hourly NO_2 Concentration
Ezamokuhle	200	68
Amersfoort		69
Daggakraal		79
Palmietfontein		89

Table 22: Annual NO_2 modelled concentrations (µg/m^3) calculated at the discrete receptors for the period 2017 to 2019

Receptor	NAAQS	Model Predicted Annual NO_2 Concentration
Ezamokuhle	40	3
Amersfoort		3
Daggakraal		4
Palmietfontein		5

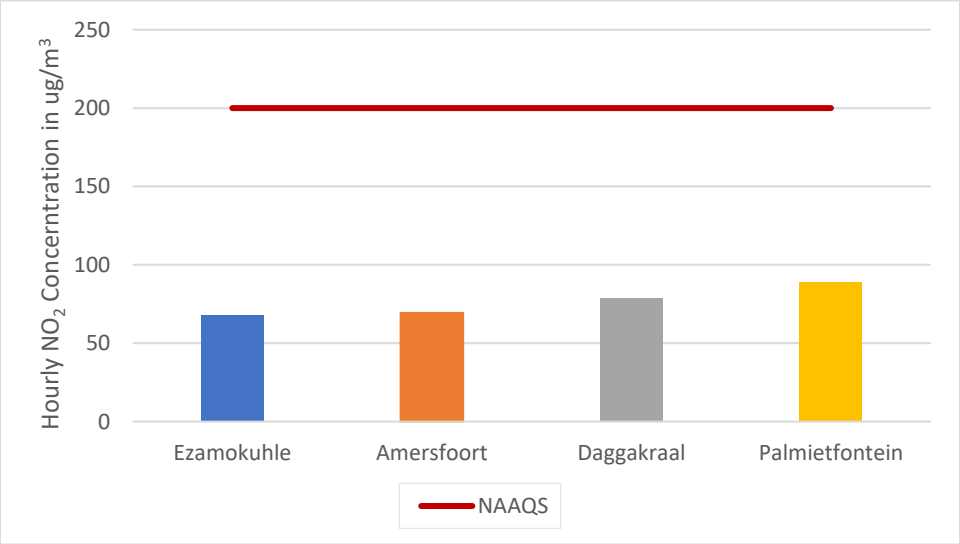

Figure 39: Hourly NO_2 99th percentile modelled concentrations (µg/m3) calculated at the discrete receptors for the period 2017 to 2019

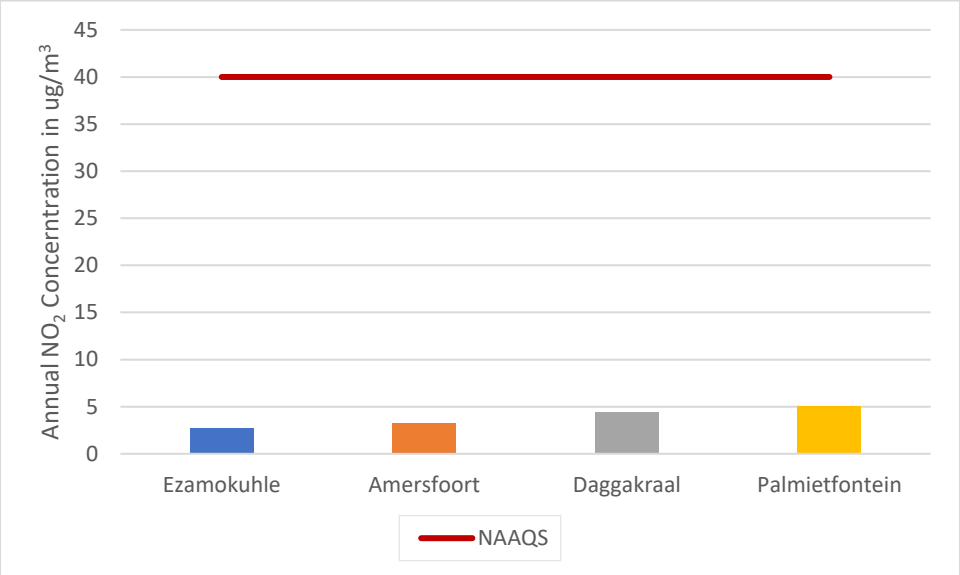

Figure 40: Annual NO_2 modelled concentrations (µg/m3) calculated at the discrete receptors for the period 2017 to 2019

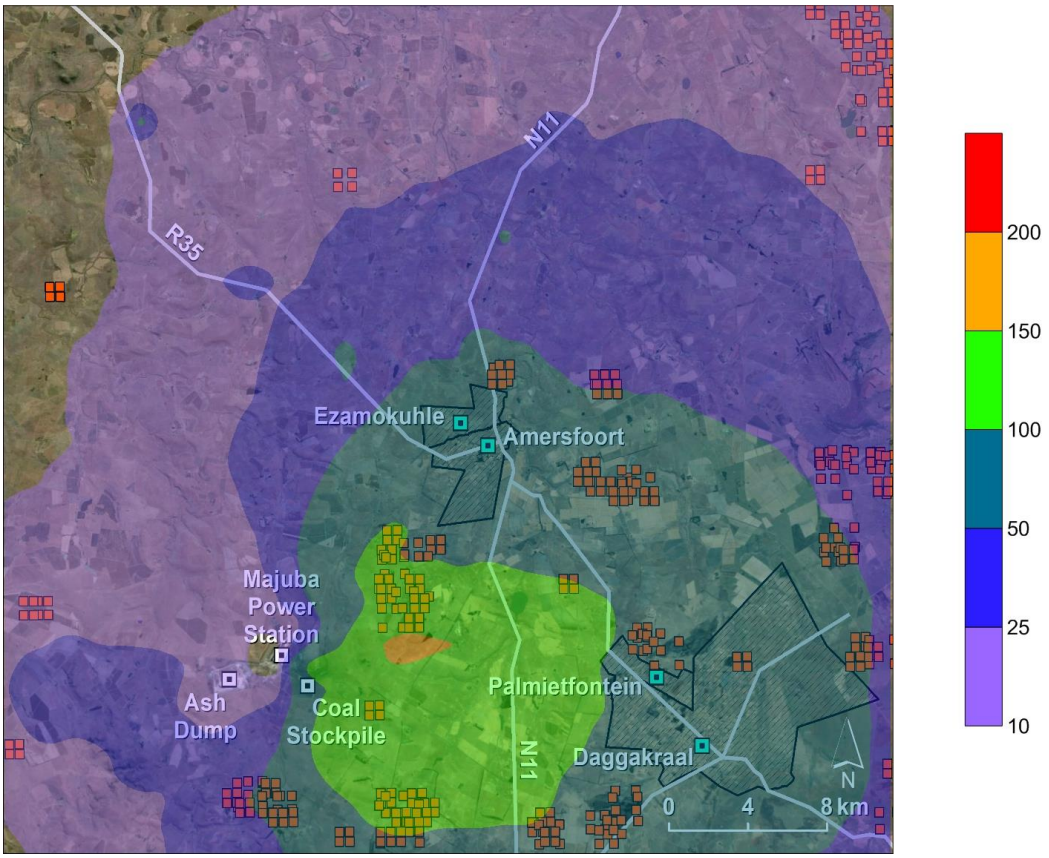

Figure 41: Hourly NO_2 99th percentile modelled concentrations (µg/m3)

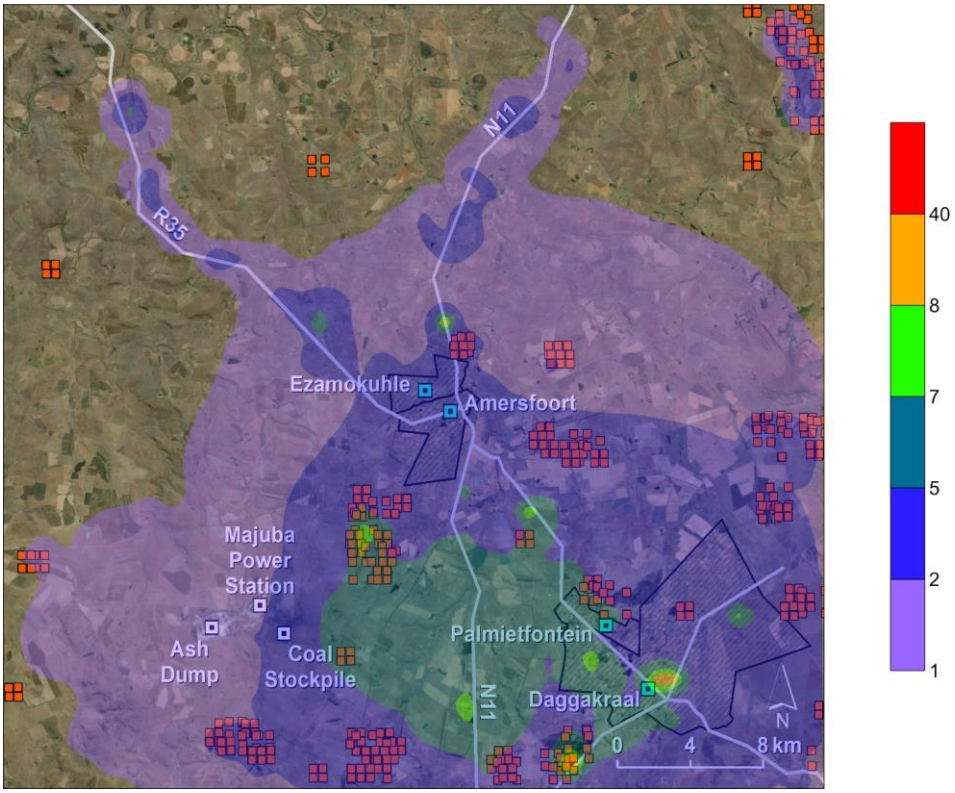

Figure 42: Annual NO_2 modelled concentrations (µg/m3)

4.1.3 PARTICULATE MATTER (PM_{10} & $PM_{2.5}$)

The model predicted 99th percentile daily and annual ambient particulate matter concentrations as a result of all emissions sources utilised in this study are generally in compliance with the NAAQS (Tables 23 to 26) at all discrete receptors (Figures 43 to 50). The particulate matter morning and afternoon peaks (Figure 12) are a typical profile for residential fuel burning. The morning peaks reduces towards midday as the inversion layer rises & improves the mixing height of the planetary boundary layer. It's evident there is a third less pronounced peak that occurs at midday (Figure 12) indicating the impact of a tall stack emission source.

Table 23: Daily PM_{10} 99th percentile modelled concentrations (µg/m^3) calculated at the discrete receptors for the period 2017 to 2019

Receptor	NAAQS	Model Predicted Daily PM_{10} Concentration
Ezamokuhle	75	8
Amersfoort		7
Daggakraal		6
Palmietfontein		8

Table 24: Daily $PM_{2.5}$ 99th percentile modelled concentrations (µg/m³) calculated at the discrete receptors for the period 2017 to 2019

Receptor	NAAQS	Model Predicted Daily $PM_{2.5}$ Concentration
Ezamokuhle	40	7
Amersfoort		6
Daggakraal		5
Palmietfontein		6

Table 25: Annual PM_{10} modelled concentrations (µg/m³) calculated at the discrete receptors for the period 2017 to 2019

Receptor	NAAQS	Model Predicted Annual PM_{10} Concentration
Ezamokuhle	40	0.90
Amersfoort		0.65
Daggakraal		0.80
Palmietfontein		1.36

Table 26: Annual $PM_{2.5}$ percentile modelled concentrations (µg/m³) calculated at the discrete receptors for the period 2017 to 2019

Receptor	NAAQS	Model Predicted Annual $PM_{2.5}$ Concentration
Ezamokuhle	20	0.64
Amersfoort		0.49
Daggakraal		0.61
Palmietfontein		0.93

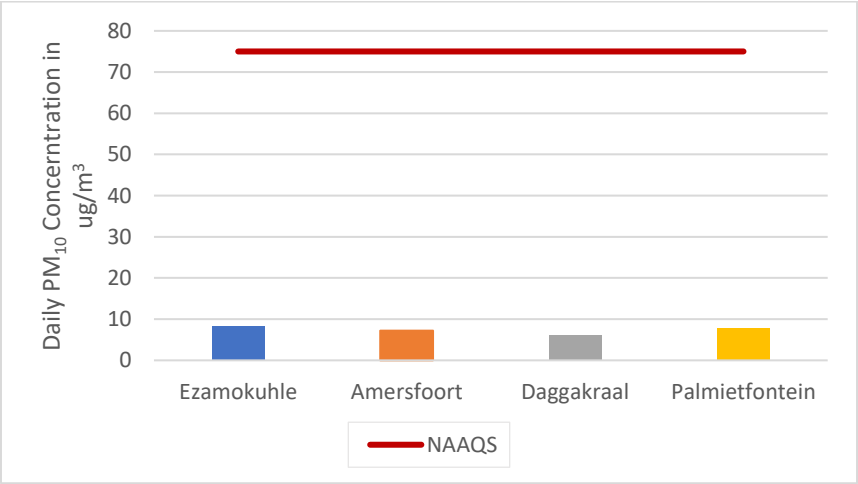

Figure 43: Daily PM_{10} 99th percentile modelled concentrations (µg/m³) calculated at the discrete receptors for the period 2017 to 2019

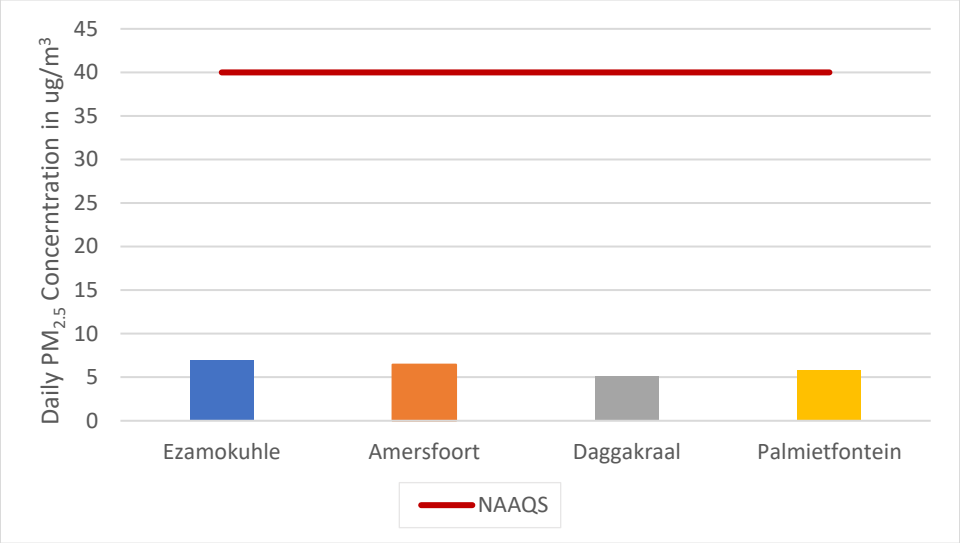

Figure 44: Daily $PM_{2.5}$ 99th percentile modelled concentrations (µg/m^3) calculated at the discrete receptors for the period 2017 to 2019

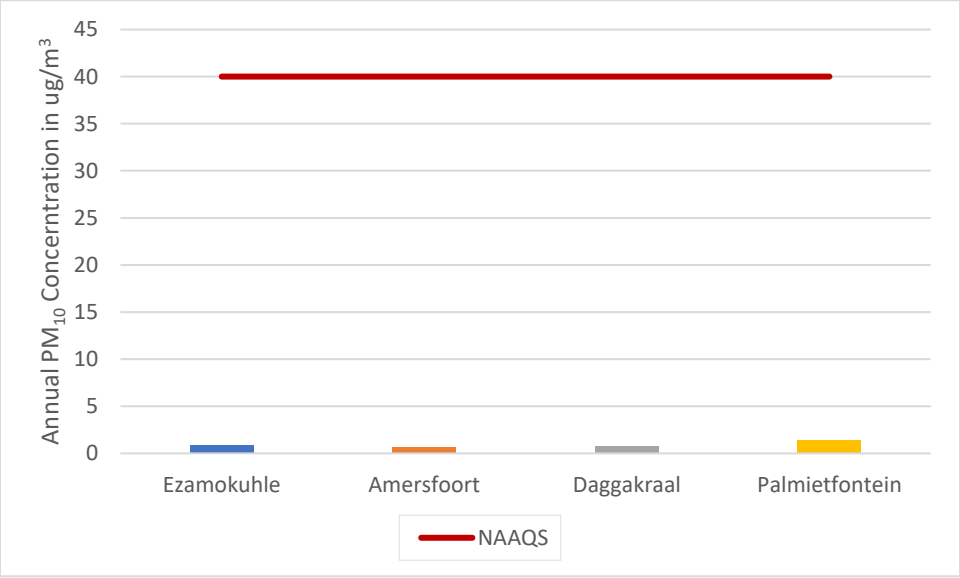

Figure 45: Annual PM_{10} modelled concentrations (µg/m^3) calculated at the discrete receptors for the period 2017 to 2019

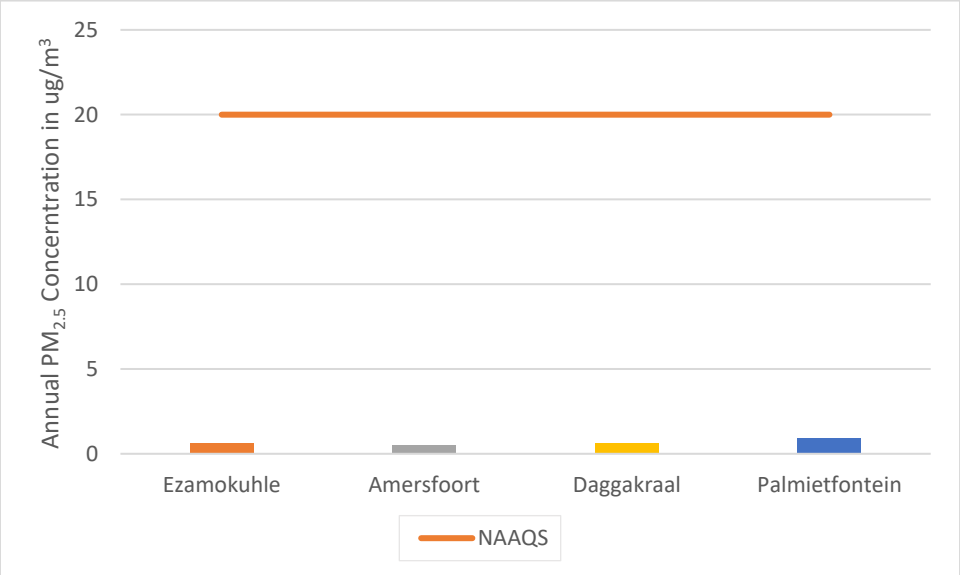

Figure 46: Annual $PM_{2.5}$ modelled concentrations (µg/m³) calculated at the discrete receptors for the period 2017 to 2019

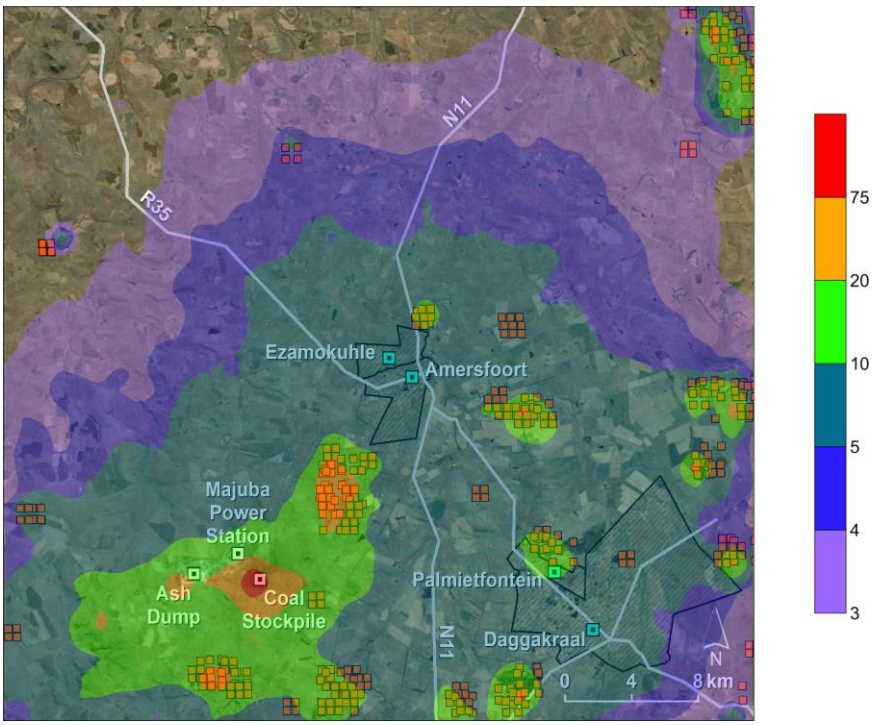

Figure 47: Daily PM_{10} 99th percentile modelled concentrations (µg/m³)

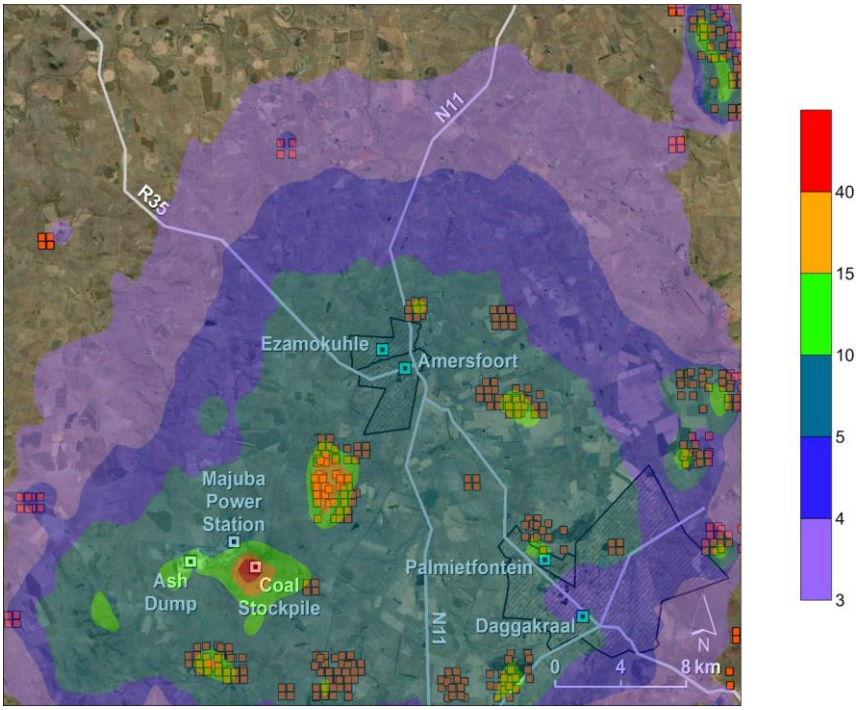

Figure 48: Daily $PM_{2.5}$ 99th percentile modelled concentrations (µg/m^3)

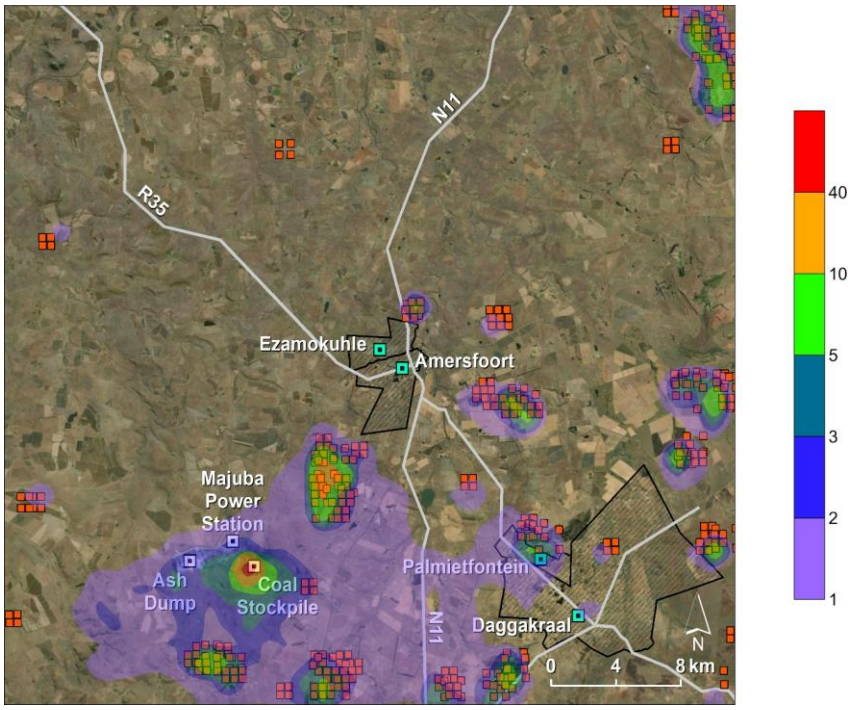

Figure 49: Annual PM_{10} modelled concentrations (µg/m^3)

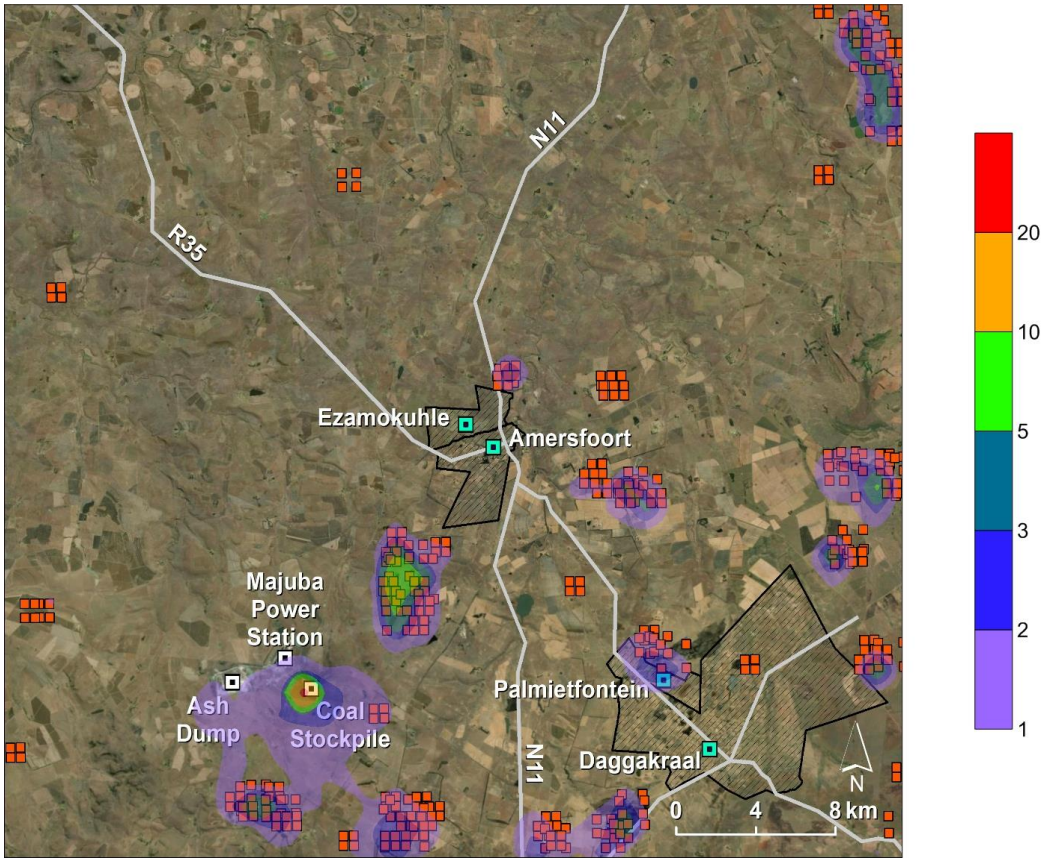

Figure 50: Annual $PM_{2.5}$ modelled concentrations (µg/m^3)

4.2 Air Quality Hotspots Identified in Ezamokuhle

The prioritisation of air quality hotspots for Ezamokuhe has been ranked on the basis of impacts. This ensures that the areas that potentially pose the greatest risk to human health and the environment are identified for placement of the E-BAM particulate analysers. Table 27 provides a summary of the model predicted daily particulate concentrations calculated at Ezamokuhle for the secondary modelling domain.

It's evident that the highest predicted concentrations occur at discrete receptors 1, 3 and 6 respectively. The discrete receptors 1 & 3 are located in China 2, Ezamokuhle whilst receptor 6 is located in Roestein, Ezamokuhle. Subsequently a total of eight air quality hotspots located in China 2 & Roestein have been identified for optimum placement of the E-BAM analysers based on the highest predicted particulate matter concentration (Figure 51 to 53). The central latitude and longitude of these eight hotspots is provided in Annexure 1.

Table 27: Daily PM_{10} & $PM_{2.5}$ 99th percentile modelled concentrations (µg/m^3) calculated at each zone for Ezamokuhle

Receptor/Zone	PM_{10}	$PM_{2.5}$
1	7.86	6.77
2	7.53	6.62
3	8.19	6.94
4	7.39	6.45
5	7.39	6.50
6	7.54	6.37
7	6.94	5.93
8	6.97	5.94
9	7.20	6.21

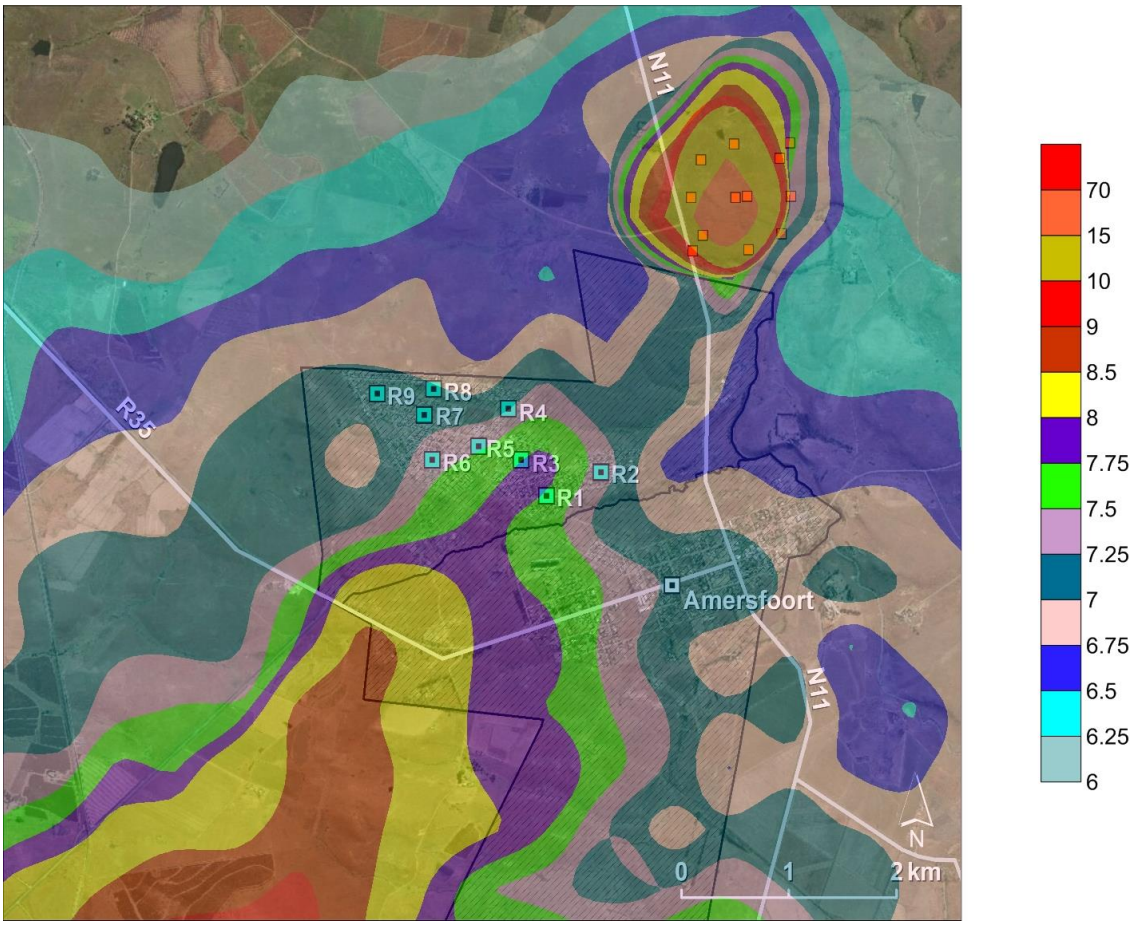

Figure 51: Daily PM_{10} 99th percentile modelled concentrations (µg/m^3) over Ezamokuhle

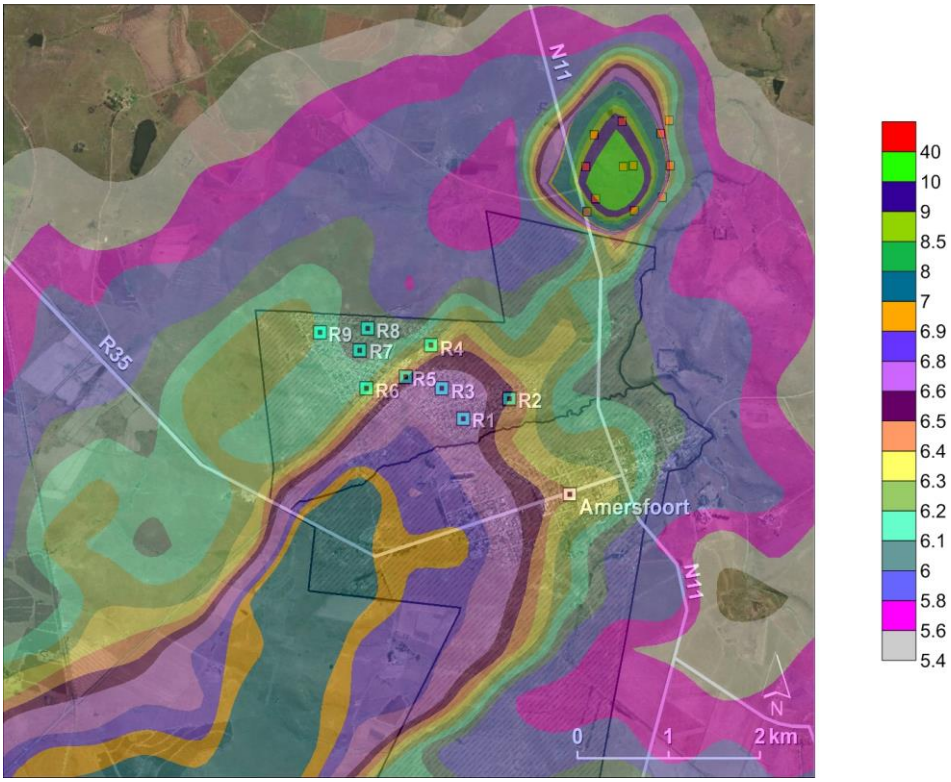

Figure 52: Daily $PM_{2.5}$ 99th percentile modelled concentrations (µg/m^3) over Ezamokuhle

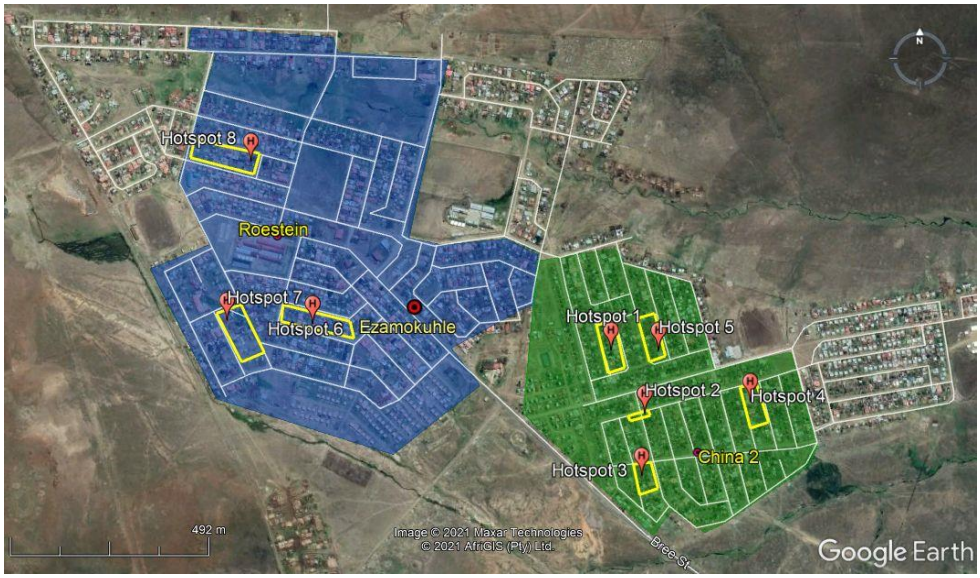

Figure 53: Air quality hotspots identified for E-BAM analyser placement

MODEL VALIDATION

Although atmospheric dispersion models are indispensable in air quality assessment studies, their limitations should always be taken into account. In this study, the model predicted concentrations arising due to cumulative baseline emissions from all sources within the modelling domain were compared to measured concentrations recorded at the Eskom Majuba and Eskom Ezamokuhle ambient monitoring stations (Figure 43). These identified deviations were then statistically analysed using the index of agreement (IOA) and the fractional bias (FB).

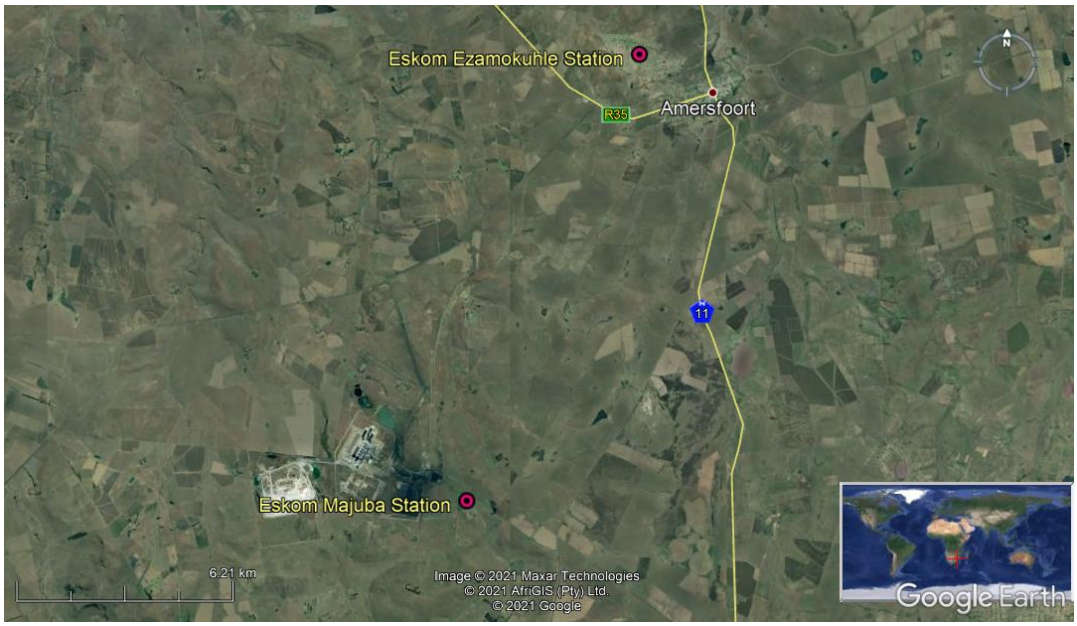

Figure 54: Location of ambient monitoring stations used for the model validation

5.2 IOA

The parameter IOA is a measure of the correlation of the predicted and observed time series of concentrations. IOA= 1[(P-O)2/(P-O) + (O-O)2] where the Predicted (P) values by the model are compared against Observed (O) data (Reza et al, 2005). The IOA varies from 0.0 (theoretical minimum) to 1.0 (perfect agreement between the observed and predicted values). An IOA with a value greater than about 0.5 is considered to be good (Hurley, 2000). The IOA's for the Eskom Majuba and Eskom Ezamokuhle are provided in Table 28.

The IOA value of the predicted and measured time series of SO_2 at the Eskom Ezamokuhle station is satisfactory (0.4). The IOA for both NO_2 and PM_{10} concentrations at the Eskom Ezamokuhle station is low at 0.2. Thus the model is under-predicting at Ezamokuhle. However it must be noted the analysis of the ambient air quality monitoring data has indicated that both NO_2 (Figure 11) and $PM_{2.5}$ (Figure 12) are dominated by non-buoyant localised ground-level sources. NO_2 (Figure 18) is conditioned by localised vehicle emissions whilst $PM_{2.5}$ is attributable to localised residential burning (Figure 19). For this study, the major roads were modelled and the local roads were excluded due to the lack of localised emissions data and similarly Stats SA data was utilised at a sub-place level to model $PM_{2.5}$ residential burning emissions. However the granularity of this data was not sufficient to cover these localised emission source catergories. It must be noted that for *Activity 12: Atmospheric Dispersion Modelling* a comprehensive emissions inventory will be developed to account for these localised sources (vehicles, local roads and residential fuel use).

For the Eskom Majuba Station, the IOA is good for $PM_{2.5}$ at 0.5, indicating a good correlation for the model predicted particulate results. The IOA is low for both NO_2 and SO_2 concentrations indicating that the model is under predicting herein, possibly due to the impact of localised and transboundary sources.

Table 28: Comparative IOA statistics between monitored data and model predictions

Pollutant	Eskom Ezamokuhle Station	Eskom Majuba Station
NO_2	0.2	0.3
SO_2	0.4	0.3
$PM_{2.5}$	0.2	0.5

5.2 FB

The FB is a measure of the agreement between the mean concentrations. The general expression for the fractional bias is given by: FB = 2 * (OB-PR)/(OB+PR), where the Observed (OB) data are compared against the Predicted (PR) values by the model (Cox & Tikvart, 1990).

The FB SO_2, NO_2 and PM_{10} ratios between the measured and predicted concentrations are shown in Table 29. The US-EPA considers the range of uncertainty in dispersion model results as being –50% to 200% in cases of extreme under and over-prediction, respectively. Model predictions falling outside of this range when compared to ambient monitored concentrations were flagged as being unrepresentative (i.e. measured to modelled ratios of <0.5 or >2.0). It evident that model under-predicted at the Eskom Ezamokuhle station whilst for the Eskom Majuba Station, the FB is good for

$PM_{2.5}$ at 0.6 which within the acceptable range. As highlighted above, the granularity of emissions inventory data was not sufficient to cover localised emission source catergories. For *Activity 12: Atmospheric Dispersion Modelling* a comprehensive emissions inventory will be developed to account for these localised sources (vehicles, local roads and residential fuel use).

Table 29: Comparative FB statistics between monitored data and model predictions

Pollutant	Eskom Ezamokuhle Station	Eskom Majuba Station
NO_2	0.03	0.4
SO_2	0.04	0.3
$PM_{2.5}$	0.003	0.6

5.3 Limitations of Study

The extent to which a user has reliable information on emissions data, meteorological data and the correct model physics set-up will influence the accuracy of the model predicted concentrations. For this baseline modelling assessment study, the following limitations must be noted:

i. Atmospheric Emission License (AEL) data serve as the principle information source for activity data in order to estimate emissions from industrial sources. Although ARM submitted a request to the Department of Environment, Forestry and Fisheries (DEFF) requesting the AEL data for industrial sources within the modelling domain, DEFF was unable to provide the data. DEFF responded stating that they will not be able to disclose the data due to data policy privacy issues. Thus the cumulative impact of other industrial sources are not included in the model simulation which results in an under prediction of the pollutants for the sector.

ii. The South African National Atmospheric Emission Inventory System (NAEIS) contains emissions info for: mines, controlled emitters and facilities identified in accordance with the local by-laws. DEFF was not able to provide ARM the NAEIS emissions data due to data policy privacy issues. Thus cumulative impact of mines, controlled emitters and facilities identified in accordance with the local by-laws are excluded from the study which results in an under prediction of the simulated pollutants.

iii. Emissions from local unpaved roads were excluded from the study. The data required to model “local roads” dust emissions are currently not available for Ezamokuhle. The information required to model these local roads includes: location of unpaved roads; silt content of each road; number of vehicles; vehicle types; empty and full weight of heavy-duty vehicles & taxis utilizing these roads. Thus the model predicted results will be under-predicted herein.

iv. Residential fuel burning for the modelling was estimated based on energy use data at the sub-place level for: Ezamokuhle utilizing StatsSa Census data. There is currently no finer resolution residential fuel burning data for Ezamokuhle as such the model simulated results are constrained by the granularity of this data. Thus the model predicted results will be under-predicted herein.

CONCLUSION

The CALPUFF modelling suite was utilised to predict the dispersion of the following pollutants: SO_2; SO_4^{2-}; NO_2; NO_3, PM_{10} and $PM_{2.5}$. The total concentrations of particulate matter (PM_{10} or $PM_{2.5}$) were computed as the sum of primary particulate matter concentrations (PM_{10} or $PM_{2.5}$) plus the contribution of concentrations from secondary particulate matter, including ammonium nitrate and ammonium sulfate. The modelled 99th percentile hourly and daily as well as the annual average modelled concentrations for SO_2, NO_2 and PM_{10} for sensitive receptors were assessed against the NAAQS. The dispersion of the pollutants were simulated for the prevailing meteorological conditions.

The model predicted 99th percentile SO_2, NO_2 and PM_{10} concentrations were generally in compliance with the NAAQS in the modelling domain. The prioritisation of air quality hotspots for Ezamokuhe was ranked on the basis of air quality impacts. This ensured that the areas that potentially pose the greatest risk to human health and the environment were identified for placement of the E-BAM particulate analysers. The highest predicted modelled concentrations for Ezamokuhle occur in China 2 and Roestein. Subsequently a total of eight air quality hotspots located in China 2 & Roestein have been identified for optimum placement of the E-BAM analysers.

The model validation exercise demonstrated that the model performance for SO_2 at the Eskom Ezamokuhle station is satisfactory whilst the model under-predicted NO_2 and PM_{10}. Although the model under-predicted at the Eskom Ezamokuhle station, the modelled performed within the acceptable range at the Eskom Majuba ambient station. Nonetheless, it must be noted that for Activity 12: Atmospheric Dispersion Modelling a comprehensive emissions inventory will be developed to account for these localised sources (vehicles, local roads and residential fuel use).

In summary, the results of this baseline modelling study has identified air quality hotspots in China 2 and Roestein for the optimum placement of the E-BAM analysers. Additionally the study has highlighted the role of non-buoyant localised ground-level sources in the Ezamokuhle airshed and the need to develop a bottom-up emissions inventory to account for these localised sources.

ACKNOWLEDGEMENTS

Air Resource Management would like to thank the following individuals for their assistance in this study

- Mr. Bryan McCourt for providing the Majuba Power Station emissions inventory;
- Mr. Maluta Mbedzi, Mr. Motshewa Matimolane & Mr. Bryan McCourt & for their technical comments on the Activity 1: Modelling Plan of Study and
- Ms. Khosi Mkongi for facilitating effective enagements with the wider Eskom team.

REFERENCES

Afrane-Okese, Y.1998. Domestic energy-use database for integrated energy planning. Unpublished MSc Thesis, Energy and Development Research Centre (EDRC), University of Cape Town.

Ainslie, B., and Jackson, P.L., 2009. The use of an atmospheric dispersion model to determine influence regions in the prince george, B.C. airshed from the burning of open wood waste piles, Journal of Environmental Management, 10, 1-9.

Alapaty, K., 1995. Sensitivity of regional oxidant model predictions to prognostic and diagnostic meteorological fields, Journal of Applied Meteorology, 34, 1787-1801.

Beychok, M. R., 2005. Fundamentals of Stack Gas Dispersion, Ch 8, 88 - 102, Irvine, California.

Busillo, G., Calastrin, G., Carpentieri, F., Matteo, A and Giovanni, G., 2005. Meteorological input for atmospheric dispersion models: an inter-comparison between new generation models, Atmospheric Environment, 8, 1212-1221.

Carslaw, D.C.,and Carslaw, N., 2007. “Detecting and characterising small changes in ur-ban nitrogen dioxide concentrations”. Atmospheric Environment Vol 41(22): pp 4723-4733.View at: http://dx.doi.org/10.1016/j.atmosenv.2007.03.034

Carslaw D.C., Ropkins K. 2012. “Openair – an r package for air quality data analysis”. Environmental Modelling and Software, pp27–28: pp52–61

Carslaw, D.“The Openair Manual Open-Source Tools for Analysing Air Pollution Data”, King’s College, London, 2015.

Davakis, E., Andronopoulos, I., Bartzisd, J.G and Nychasa, S.G., 2007. Data assimilation in meteorological pre-processors: Effects on atmospheric dispersion simulations. Atmospheric Environment, 41, 2917–2932

DEFF (2007): The Vaal Triangle Priority Area Air Quality Management Plan – Baseline Characterisation.

DEFF (2013): Integrated Strategy for the control of Motor Vehicle Emissions: Motor Vehicle Emission Inventory.

DEFF (2019): The Second Generation Vaal triangle Airshed Priority Area Air Quality Management Plan- (URL: https://saaqis.environment.gov.za/NewsPage/CorrentNew/21)

Garstang, M., Tyson, P.D., Swap, R., Edwards, M., Kållberg, P. and Lindesay, J.A. (1996). Horizontal and vertical transport of air over Southern Africa. Journal of Geophysical Research, 101 (D19), 23721-23736.

Grundstrom, M., Tang, L., Hallquist, M., Nguyen, H., Chen, D., and Pleijel,H. "Influence of atmospheric circulation patterns on urban air quality during the winter" Atmospheric Pollution Research,Vol 6(2), pp 278-285. View at: https://doi.org/10.5094/APR.2015.032.

Holmes, N.S. and Morawska, L., 2006. A review of dispersion modelling and its application to the dispersion of particles: An overview of different dispersion models available, Atmospheric Environment, 40, 5902–5928.

Hurley, P.J., Physick, W.L. and Luhar, A.K., 2005a. TAPM: a practical approach to prognostic meteorological and air pollution modelling. Environmental Modelling & Software, 20, 737-752.

Hurley, P., Physick, W., Luhar, A. and Edwards, M., 2005b. The Air Pollution Model (TAPM) Version 3. Part 2: Summary of some verification studies. CSIRO Atmospheric Research, 72, 20-36.

Hurley, P.J., 2005c: The Air Pollution Model (TAPM) Version 3 Part 1: Technical Description. www.dar.csiro.au/tapm

Hurley, P.J., Edwards, M., Physick, W.L. and Luhar, A.K., 2005. TAPM V3 – Model Description and Verification , Clean Air and Environmental Quality, 39, 7-15.

Hurley, P., Manins, P., Lee, S., Boyle, R., Leung, Y. and Dewundege, P., 2003. Year-long, high-resolution, urban airshed modelling: verification of TAPM predictions of smog and particles in Melbourne, Australia, Atmospheric Environment, 37, 1899–1910

Jones, A.M., Harrison, R.M., Baker, J., 2010. "The wind speed dependence of the concentrations of airborne particulate matter and nox". Atmospheric Environment Vol 44(13), pp 1682-1690. View at:http://www.sciencedirect.com/science/article/B6VH3-4Y7P72C-2/2/f6c65e5f49ac3e9862d4c1803d4735c0.

Liebenberg, H., 1999. "Air pollution population exposure evaluation in the Vaal triangle using GIS" (Doctoral dissertation, University of Johannesburg).

Pielke, R.A., Uliasz, M., 1998. Use of meteorological models as input to regional and mesoscale air quality models limitations and strengths, Atmospheric Environment 32, 1455–1466

Richard Reiss, Elizabeth L. Anderson, Carroll E. Cross, George Hidy, David Hoel, Roger McClellan & Suresh Moolgavkar (2007) Evidence of Health Impacts of Sulfate-and Nitrate-Containing Particles in Ambient Air, Inhalation Toxicology, 19:5, 419-449, DOI: 10.1080/08958370601174941

Sandberg , D.A. Levaggi , R.E. DeMandel & W. Siu (1976) Sulfate and Nitrate Particulates as Related to SO2 and NOX Gases and Emissions, Journal of the Air Pollution Control Association, 26:6, 559-564, DOI: 10.1080/00022470.1976.10470283

Scire J (2014). Peer Review Report on the approach to the Atmospheric Impact Report https://docs.srk.co.za/sites/default/files/File/South-Africa/publicDocuments/SASOL_Postponements/ANNEXURE_B_SYNFUELS_AIR_Peer_Review.pdf

South African National Biodiversity Institute (2004): National Spatial Biodiversity Assessment

Scott, G.M., Diab, R.D., 2000. Forecasting Air Pollution Potential: A synoptic climatological approach, Journal of Air and Waste Management Association, 50, 1831-1842.

Scire, J.S., Robe, F., Yamartino, R.J., 1999a. A User's Guide for the CALMET Meteorological Model (Version 5). Earth Tech, Concord.

Scire, J.S., and Robe, F., 2004. Evaluating performance of meteorological models in regulatory application studies, oral presentation at the 8th International Conference on Harmonisation within Atmospheric Dispersion Modelling for Regulatory Purposes.

Swap, R., Garstang, M., Macko, S.A., Tyson, P.D., Maenhaut, W., Artaxo, P., Kallberg, P. and Talbot, R. (1999). The long-range transport of southern African aerosols to the tropical south Atlantic. Journal of Geophysical Research, 101 (D19), 23777-23791.

US Environmental Protection Agency., 2005. 40 CFR Part 51 Revision to the Guideline on Air Quality Models: Adoption of a Preferred General Purpose (Flat and Complex Terrain) Dispersion Model and Other Revisions; Final Rule Appendix W (PDF), Extracts from the Guideline on Air Quality Models.

Zawar, P., Reza, T., Kingham, S. and Pearce, J., 2005. Evaluation of a year- long dispersion modelling of PM10 using the mesoscale model TAPM for Christchurch, New Zealand, Science of the Total Environment, 349, 249– 259.

Zunckel, M.,2007c. Air quality modelling activities in Southern Africa and the feasibility of a regional modelling centre, Report done on behalf of APINA.

ANNEXURE 1

The central latitude and longitude for the eight air quality hotspots is shown in Table 28.

Table 30: GPS co-ordinates for Air Quality Hotspots

Area	Household	Latitude	Longitude
China 2	1	27° 0'1.01"S	29°51'12.03"E
	2	27° 0'6.09"S	29°51'15.00"E
	3	27° 0'11.05"S	29°51'14.66"E
	4	27° 0'5.24"S	29°51'24.49"E
	5	27° 0'1.07"S	29°51'16.30"E
Roestein	6	26°59'58.61"S	29°50'45.25"E
	7	26°59'58.28"S	29°50'37.56"E
	8	26°59'45.60"S	29°50'39.88"E

ANEXURE 2

REPORT DISCLAIMER

Air Resource Management (Pty) Ltd has prepared this report based on an agreed scope of work and acts in all professional matters as an advisor to the Client and exercises all reasonable skill and care in the provision of its professional services in a manner consistent with the level of care and expertise exercised by air quality management professionals.

Reports are commissioned by and prepared for the exclusive use of the Client. They are subject to and issued in accordance with the agreement between the Client and Air Resource Management (Pty) Ltd. Air Resource Management (Pty) Ltd is not responsible and will not be liable to any other person or organisation for or in relation to any matter dealt within this Report, or for any loss or damage suffered by any other person or organisation arising from matters dealt with or conclusions expressed in this report (including without limitation matters arising from any negligent act or omission of Air Resource Management (Pty) Ltd or for any loss or damage suffered by any other party relying upon the matters dealt with or conclusions expressed in this Report). Other parties should not rely upon the report or the accuracy or completeness of any conclusions and should make their own inquiries and obtain independent advice in relation to such matters.

Except where expressly stated, Air Resource Management (Pty) Ltd has not verified the validity, accuracy or comprehensiveness of any information supplied to Air Resource Management (Pty) Ltd for its reports.

Reports prepared by Air Resource Management (Pty) Ltd cannot be copied or reproduced in whole or part for any purpose without the prior written agreement of Air Resource Management (Pty) Ltd.

Where site inspections, testing or fieldwork have taken place, the report is based on the information made available by the client or their nominees during the visit, visual observations and any subsequent discussions with regulatory authorities. The validity and comprehensiveness of supplied information has not been independently verified and, for the purposes of this report, it is assumed that the information provided to Air Resource Management (Pty) Ltd is both complete and accurate. It is further assumed that normal activities were being undertaken at the site on the day of the site visit(s), unless explicitly stated otherwise.

COPYRIGHT